

1 **Positively selected effector genes and their contribution to virulence in the smut fungus**  
2 ***Sporisorium reilianum***

3  
4 Gabriel Schweizer<sup>1</sup>, Karin Münch<sup>1</sup>, Gertrud Mannhaupt<sup>1,2</sup>, Jan Schirawski<sup>1,3</sup>, Regine  
5 Kahmann<sup>1\*</sup> and Julien Y. Dutheil<sup>1,4,5\*</sup>

6  
7 <sup>1</sup>Max-Planck-Institute for Terrestrial Microbiology, Department of Organismic Interactions,  
8 Karl von Frisch-Straße 10, 35043 Marburg, Germany.

9  
10 <sup>2</sup>Helmholtz Zentrum München, Institute for Bioinformatics and Systems Biology, Ingolstädter  
11 Landstraße 1, 85764 Neuherberg, Germany.

12  
13 <sup>3</sup>Current address: RWTH Aachen, Institute of Applied Microbiology, Microbial Genetics,  
14 Worringer Weg 1, 52074 Aachen, Germany.

15  
16 <sup>4</sup>University of Montpellier 2, Institute of Evolutionary Sciences of Montpellier, Place Eugène  
17 Bataillon, 34095 Montpellier, France.

18  
19 <sup>5</sup>Current address: Max-Planck-Institute for Evolutionary Biology, Research Group Molecular  
20 Systems Evolution, August-Thienemann-Straße 2, 24306 Plön, Germany.

21  
22  
23 \* Authors for correspondence:

24  
25 Dr. Julien Y. Dutheil  
26 Max-Planck-Institute for Evolutionary Biology  
27 Research Group Molecular Systems Evolution  
28 August-Thienemann-Straße 2  
29 24306 Plön  
30 Germany  
31 Phone: +49 4522 763 298  
32 Fax: +49 4522 763 281  
33 Email: [dutheil@evolbio.mpg.de](mailto:dutheil@evolbio.mpg.de)

34  
35 Prof. Dr. Regine Kahmann  
36 Max-Planck-Institute for Terrestrial Microbiology  
37 Department of Organismic Interactions  
38 Karl-von-Frisch Straße 10  
39 35043 Marburg  
40 Germany  
41 Phone: +49 6421 178 501  
42 Fax: +49 6421 178 509  
43 Email: [kahmann@mpi-marburg.mpg.de](mailto:kahmann@mpi-marburg.mpg.de)

44  
45  
46

47 **Abstract**

48 Plants and fungi display a broad range of interactions in natural and agricultural ecosystems  
49 ranging from symbiosis to parasitism. These ecological interactions result in coevolution  
50 between genes belonging to different partners. A well-understood example are secreted fungal  
51 effector proteins and their host targets, which play an important role in pathogenic  
52 interactions. Biotrophic smut fungi (Basidiomycota) are well-suited to investigate the  
53 evolution of plant pathogens, because several reference genomes and genetic tools are  
54 available for these species. Here, we used the genomes of *Sporisorium reilianum* f. sp. *zear*  
55 and *S. reilianum* f. sp. *reilianum*, two closely related formae speciales infecting maize and  
56 sorghum, respectively, together with the genomes of *Ustilago hordei*, *Ustilago maydis* and  
57 *Sporisorium scitamineum* to identify and characterize genes displaying signatures of positive  
58 selection. We identified 154 gene families having undergone positive selection during species  
59 divergence in at least one lineage, among which 77% were identified in the two investigated  
60 formae speciales of *S. reilianum*. Remarkably, only 29% of positively selected genes encode  
61 predicted secreted proteins. We assessed the contribution to virulence of nine of these  
62 candidate effector genes in *S. reilianum* f. sp. *zear* by deleting individual genes, including a  
63 homologue of the effector gene *pit2* previously characterized in *U. maydis*. Only the *pit2*  
64 deletion mutant was found to be strongly reduced in virulence. Additional experiments are  
65 required to understand the molecular mechanisms underlying the selection forces acting on  
66 the other candidate effector genes, as well as the large fraction of positively selected genes  
67 encoding predicted cytoplasmic proteins.

68

69 **Keywords**

70 Positive selection; effector evolution; smut fungi; comparative genomics; virulence

71

72

### 73 **Introduction**

74 Plants and fungi have a long history of coevolution since the emergence of pioneering land  
75 plants approximately 400 million years ago. The development of early plants was likely  
76 supported by associations with symbiotic fungi, as suggested by analyses of ribosomal RNAs  
77 and fossil records (Remy et al. 1994; Gehrig et al. 1996; Martin et al. 2017). Different forms  
78 of plant-fungus interactions have evolved, including mutualistic symbiosis where both plant  
79 and fungus benefit (Parniske 2008), and pathogenic interactions where fungal colonization  
80 greatly reduces plant fitness (Dean et al. 2012). Pathogenic interactions play critical roles in  
81 natural and agricultural ecosystems, and understanding the evolutionary mechanisms shaping  
82 them is of great importance to plant production, food security and protection of biodiversity in  
83 natural ecosystems (Fisher et al. 2012; Bagchi et al. 2014).

84 Secreted fungal effector proteins are key players in pathogenic interactions as they are  
85 involved in protecting and shielding growing hyphae, suppressing plant defense responses and  
86 changing plant physiology to support growth of the pathogen (Stergiopoulos and de Wit 2009;  
87 de Jonge et al. 2011; Giraldo and Valent 2013). Many effector proteins lack known functional  
88 domains, and expression of a subset of effectors is linked to plant colonization (Lo Presti et al.  
89 2015; Toruño et al. 2016; Franceschetti et al. 2017; Lanver et al. 2017). Effector proteins with  
90 a strong effect on virulence phenotype are thought to coevolve with their plant targets either  
91 in an arms race or a trench-warfare scenario (Brown and Tellier 2011). In the former, fungal  
92 effectors manipulating the host are under positive directional selection, and plant targets  
93 evolve in response to changes in effector proteins (Rovenich et al. 2014). In the latter  
94 scenario, sets of alleles are maintained by balancing selection in both host and pathogen  
95 populations (Brown and Tellier 2011; Tellier et al. 2014). Several methods are available for  
96 identifying genomic regions under selection (Nielsen 2005; Aguileta et al. 2009; Aguileta et

97 al. 2010). It has been proposed that genes with signatures of positive selection have important  
98 functions during host pathogen interaction or have contributed to host specialization (Tiffin  
99 and Moeller, 2006). It is therefore expected that the deletion of such genes reduces virulence  
100 when tested on a susceptible host.

101 Depending on the aim of the investigation, studies identifying genes with signatures of  
102 positive selection are carried out within or between species. Whilst studies on the population  
103 level focus on recent and ongoing selective processes and are instrumental in the  
104 understanding of adaptation, comparative genomic studies employing different species  
105 encompass a broader time span and provide insight into the underlying genetic basis of host  
106 specialization (Plissonneau et al. 2017). The signature of positive selection in such case  
107 typically takes the form of an excess of divergence between species due to increased fixation  
108 of mutations by selective sweeps compared to a neutral expectation (Yang and Nielsen,  
109 1998). This is commonly measured by the ratio of non-synonymous ( $d_N$ ) over synonymous  
110 ( $d_S$ ) divergence and a  $d_N / d_S$  ratio  $> 1$  is taken as evidence for positive selection under the  
111 assumption that synonymous substitutions are neutral while non-synonymous are not. Positive  
112 selection studies in a number of plant pathogen systems revealed that genes encoding secreted  
113 effector proteins are enriched in signatures of positive selection (Möller and Stukenbrock  
114 2017). Such studies include investigations in diverse plant pathogens like *Microbotryum*  
115 species causing anther-smut disease of Caryophyllaceae species (Aguileta et al. 2010), the  
116 wheat pathogen *Zymoseptoria tritici* (Stukenbrock et al. 2011), the rust fungus *Melampsora*  
117 *larici-populina* (Hacquard et al. 2012), the rice blast fungus *Magnaporthe oryzae* (Huang et  
118 al. 2014), the wheat stem rust fungus *Puccinia graminis* f. sp. *tritici* (Sperschneider et al.  
119 2014) the Irish potato famine pathogen *Phytophthora infestans* (Dong et al. 2014), a group of  
120 *Fusarium* species (Sperschneider et al. 2015) and a group of smut fungi parasitizing different  
121 grasses and a dicot host (Sharma et al. 2014; Sharma et al. 2015). Yet, as only a few genes

122 under positive selection have been functionally studied, the link between the selected  
123 genotypes and their corresponding phenotypes are only beginning to be understood and only a  
124 few studies used evolutionary predictions to unravel the molecular mechanisms of host  
125 adaptation. For example, the population genomics study in the wheat pathogen *Z. tritici* which  
126 identified candidate effector genes under positive selection (Stukenbrock et al. 2011) was  
127 followed up experimentally, and in this case it was shown that the deletion of three of four  
128 candidate genes reduced virulence (Poppe et al. 2015). In the grey mold fungus *Botrytis*  
129 *cinerea* four positively selected genes were deleted without affecting virulence, and this  
130 finding was attributed to functional redundancy, the limited number of tested host plants, or  
131 experimental conditions different from natural infections (Aguileta et al. 2012). A study of the  
132 oomycete effector protein EpiC1 showed that a single amino acid substitution at a site under  
133 positive selection affected the binding affinity of different host proteases determining host  
134 specificity (Dong et al. 2014).

135 Smut fungi, belonging to the division of Basidiomycota, are a group of about 550 species  
136 parasitizing mostly grasses, including important crops like maize, sorghum, oat, barley and  
137 sugarcane (Begerow et al. 2014). In smut fungi, sexual reproduction is linked to pathogenic  
138 development and smut fungi therefore depend on successful plant colonization to complete  
139 their life cycle. As biotrophic pathogens, they require living plant tissue for establishing a  
140 successful interaction (Martinez-Espinoza et al. 2002). With few exceptions like *Ustilago*  
141 *maydis*, smut fungi usually develop symptoms only in the female or male inflorescence of  
142 their respective host plants. During the last ten years, quality draft genome sequences of  
143 prominent species were obtained, including *U. maydis*, the causative agent of smut disease on  
144 maize and teosinte (Kämper et al. 2006), *Sporisorium reilianum* causing head smut of maize  
145 and sorghum (Schirawski et al. 2010), *Ustilago hordei* infecting barley (Laurie et al. 2012),  
146 and *Sporisorium scitamineum* parasitizing sugarcane (Que et al. 2014; Taniguti et al. 2015;

147 Dutheil et al. 2016). The head smut fungus *S. reilianum* occurs in two formae speciales that  
148 infect maize (*S. reilianum* f. sp. *zuae*) or sorghum (*S. reilianum* f. sp. *reilianum*) (Zuther et al.  
149 2012). The concept of formae speciales is used in phytopathology to distinguish members of  
150 the same species based on their ability to colonize a certain host plant (in this example maize  
151 or sorghum) (Anikster, 1984). The divergence of *U. hordei*, *U. maydis*, *S. scitamineum* and *S.*  
152 *reilianum* was inferred to have occurred in the interval of seven and 50 million years ago  
153 (Munkacsi et al. 2007). The availability of genome sequences of several species with different  
154 host ranges, together with established tools for genetic manipulations (Brachmann et al. 2004;  
155 Kämper 2004; Khrunyk et al. 2010; Schuster et al. 2016) make this group of smut fungi  
156 particularly interesting to study the evolution of effector genes as well as their contributions to  
157 virulence, speciation and host specificity.

158 Here, we employed the genome of the recently sequenced strain *S. reilianum* f. sp. *reilianum*  
159 SRS1\_H2-8 (<http://www.ebi.ac.uk/ena/data/view/LT795054-LT795076>) (Zuther et al. 2012)  
160 together with the genomes of *U. maydis*, *U. hordei*, *S. scitamineum* and *S. reilianum* f. sp.  
161 *zuae* to identify potential effector genes with signatures of positive selection. Candidate genes  
162 were individually deleted in *S. reilianum* f. sp. *zuae* and the phenotype of the deletion strains  
163 was assessed after infection of maize in order to understand their function with respect to  
164 virulence. We report that the deletion of one candidate gene, *pit2*, led to a strong reduction in  
165 virulence and we further discuss hypotheses on the origin of positive selection for the other  
166 candidate genes.

167

168

## 169 **Materials and Methods**

170 *Construction of homologous protein families*

171 Fungal species used in this study, their number of gene models, number of predicted secreted  
172 proteins and sources of genome data are listed in supplementary table S1. The predicted  
173 proteome of the five smut fungi *U. hordei*, *U. maydis*, *S. scitamineum*, *S. reilianum* f. sp. *zeae*  
174 and *S. reilianum* f. sp. *reilianum* were used to perform an all-against-all blastp search  
175 (Altschul et al. 1990). The SiLiX algorithm was subsequently used to infer homology  
176 relationships based on the blast hits (Miele et al. 2011). Two parameters are considered to  
177 decide whether a Blast hit can be taken as evidence for homology: the percent identity  
178 between two sequences and the relative length of the hit compared to the total length of the  
179 two sequences, hereby referred to as “coverage”. In order to maximize the number of families  
180 comprising 1:1 orthologues (that is families that have an equal number of members in each  
181 species), SiLiX (Miele et al. 2011) was run with a range for coverage and identity thresholds  
182 between 5 % and 95 % in 5 % steps. An identity of 40 % and coverage between 5 % and 45 %  
183 lead to the maximum number of families with 1:1 orthologues (5,394; supplementary fig. S1)  
184 while settings with 40 % identity and 80 % coverage lead to 5,326 families with 1:1  
185 orthologues (supplementary fig. S1). Since using a higher coverage had only a cost of 68 core  
186 families, the stricter criteria were applied for family clustering. Families with at least two  
187 members were aligned on the codon level using MACSE 1.01b (Ranwez et al. 2011) and on  
188 the protein level using PRANK v.100802 (Löytynoja and Goldman 2008). The resulting  
189 alignments were subsequently compared and column scores (CS) computed for each position  
190 in the alignment (Thompson et al. 1999). Only positions with CS of 100 % (that is, alignment  
191 columns identically found by both methods) and a maximum of 30 % gaps were retained for  
192 further analysis.

193

194 *Estimation of genome-wide divergence values and divergence times*

195 The five genomes of *U. hordei*, *U. maydis*, *S. scitamineum*, *S. reilianum* f. sp. *zeae* and *S.*  
196 *reilianum* f. sp. *reilianum* were aligned using the Multiz genome aligner from the TBA  
197 package (Blanchette et al. 2004) and projected on the *U. maydis* genome as reference. The  
198 resulting multiple genome alignment had a total size of 21 Mb and was further restricted to  
199 regions with homologous sequences in the five species (total length after this step: 14.3 Mb)  
200 and processed to remove coding regions. The final non-coding sequence alignment had a  
201 total length of 2.2 Mb, for which pairwise nucleotide similarities were computed in non-  
202 overlapping windows of 10 kb.

203 Gene families with exactly one member in each species were concatenated and pairwise  
204 protein sequence similarities computed using the *seqinr* package for R (Charif and Lobry  
205 2007). Protein alignments were also used to infer dates of divergence, using a relaxed clock  
206 model. The PhyloBayes version 4.1 software (Lartillot et al. 2009) was used with the auto-  
207 correlated model of Thorne et al. (Thorne et al. 1998) under a GTR + CAT model. A unique  
208 calibration point was used, based on the divergence time of the most divergent lineage *U.*  
209 *hordei*, previously estimated to have occurred between 27 and 21 Myr (Bakkeren and  
210 Kronstad, 2007). A uniform prior was used on this interval for the Monte-Carlo Markov  
211 Chain. As convergence issues arise when large alignments (more than 20,000 positions) are  
212 used, we followed the PhyloBayes authors' recommendation to conduct a jackknife  
213 procedure. We generated three datasets of ca 20,000 amino acids by randomly sampling  
214 families and concatenating the corresponding alignments. Two chains were run in each case  
215 and convergence was assessed. Sampling was performed after a burning of 10,000 iterations,  
216 and every 10 subsequent iterations. Chains were run to ensure that the minimum effective  
217 sample size was greater than 50 and maximum relative difference lower than 0.3 in at least  
218 one sample. Results are summarized in supplementary table S2 and supplementary fig. S2  
219 shows the six chains for the three samples. In addition to the convergence of the two chains



220 for each sample, our results reveal extremely consistent results between samples. Figure 1A  
221 shows estimates from one chain of the third data set, which shows a minimum effective  
222 sample size greater than 300.

223

224

225

### 226 *Detection of positive selection*

227 For gene families with at least three members, translated sequences were employed to create  
228 maximum likelihood phylogenetic trees using PhyML 3.0 (Guindon et al. 2010) with a  
229 minimum parsimony starting tree and the LG amino acid substitution model with a four-  
230 classes gamma distribution of site-specific substitution rate (Le and Gascuel 2008). The best  
231 tree topology obtained from nearest neighbor interchange (NNI) and subtree pruning  
232 recrafting (SPR) searches was kept (Guindon et al. 2010). BppML (Dutheil and Boussau  
233 2008) was then used to re-estimate branch lengths from the codon alignment using the YN98  
234 substitution model (Nielsen and Yang 1998). We next aimed at inferring the occurrence of  
235 positive selection for each gene family. This is typically achieved by measuring the ratio of  
236 non-synonymous vs. synonymous substitutions ( $d_N/d_S$  ratio) using models of codon sequence  
237 evolution (Yang, 2006). In particular, non-homogeneous models of sequence evolution  
238 estimate the  $d_N/d_S$  ratio independently in different lineages, yet at the cost of potential over-  
239 parametrization issues. In the manual of the PAML package, the authors state that such  
240 models should only be used for hypothesis testing and advise against using them for scans of  
241 positive selection. Dutheil et al. (2012) proposed a model selection approach (implemented in  
242 the TestNH package) allowing to select for the best non-homogeneous model supported by  
243 the data. They start by fitting the simplest (homogeneous) model and sequentially add  
244 parameters to model variation of selective regime among lineages. Because the number of

245 possible models is large even for small data sets, two heuristic approaches have been  
246 introduced: the ‘free’ heuristic permits unconnected branches from the tree to evolve under  
247 the same regime, while the ‘joint’ heuristic restricts model sharing to connected branches (see  
248 Dutheil et al. 2012 for details). The choice of models to test is guided by statistics on the  
249 patterns of substitutions on the phylogenetic tree, an approach named *substitution mapping*  
250 (Romiguier et al. 2012). Apart from the model selection approach, the underlying models of  
251 codon sequence evolution are identical to the one originally described by Yang (Yang, 1998;  
252 Yang and Nielsen, 1998). Model selection was performed with the TestNH software, which  
253 contains two programs: (1) MapNH (Romiguier et al. 2012) was used for mapping  
254 substitutions on the previously inferred phylogenetic tree and (2) PartNH (Dutheil et al. 2012)  
255 was subsequently employed to fit time non-homogeneous models of codon substitutions.  
256 PartNH uses the previously inferred substitution maps in order to perform model comparisons  
257 and select a non-homogeneous model with minimal number of parameters. Both methods  
258 ‘free’ and ‘join’ were applied and compared to scan for positive selection. Finally, putative  
259 secreted effector proteins were identified by predicting secretion using SignalP 4.0 (Petersen  
260 et al. 2011) and proteins were considered as secreted if the program indicated the presence of  
261 a signal peptide but no transmembrane domain.

262 To detect residues under positive selection in homologues of *pit2*, the branch-site model with  
263 Bayes Empirical Bayes (BEB) analysis as implemented in PAML4 (Yang 2007) was applied.  
264 We employed information about family composition, alignment and phylogeny as outlined  
265 above and defined *sr10529* and *srs\_10529* as foreground branches. A posterior probability  
266 threshold of > 95 % was used for the BEB analysis.

267

268 *Association of positively selected genes with repeats in U. hordei*

269 We tested whether genes under positive selection are located significantly closer to repetitive  
270 elements than average genes in the genome of *U. hordei*, which shows the highest content of  
271 repetitive elements in the group of smut fungi investigated here. For this analysis, only a  
272 group of “uncharacterized interspersed repeats” was investigated, because it was shown  
273 previously that this is the only category showing a strong association with candidate effector  
274 genes (Dutheil et al. 2016). Binary logistic regressions were conducted in R using the *rms*  
275 package (Harrell 2015). The ‘robcov’ function of the *rms* package was used in order to get  
276 robust estimates of each effect. The variable “distance to the closest interspersed repeat” was  
277 transformed by  $\log(x+1)$  because of its extreme distribution.

278

#### 279 *Comparing $d_N/d_S$ ratios of genes residing in virulence clusters*

280 Previous work has identified several virulence gene clusters in *U. maydis* and some of them  
281 play important roles during pathogenic development (Kämper et al. 2006; Schirawski et al.  
282 2010). In total, these clusters contain 163 genes, where 100 reside in clusters without  
283 virulence phenotype and 63 reside in clusters with virulence phenotype upon deletion. Both  
284 types of clusters contain each 32 genes for which a  $d_N/d_S$  ratio could be determined (the  
285 missing genes are part of families that do not have at least three members and were therefore  
286 not analyzed). The  $d_N/d_S$  ratios of all genes in clusters were compared between clusters with  
287 and without virulence phenotype (Wilcoxon Rank-Sum Test).

288

#### 289 *Gene Ontology terms enrichment analysis*

290 All proteins in *S. reilianum* f. sp. *zeae*, in *S. reilianum* f. sp. *reilianum* and in *U. hordei* were  
291 considered for Gene Ontology (GO) term enrichment analyses. GO terms were assigned using  
292 iprscan 1.1.0 (<http://fgblab.org/runiprscan>; developed by Michael R. Thon) which links GO  
293 information provided by Interpro to each protein. In this way, 1,759 unique GO terms could

294 be assigned to 4,130 proteins in *S. reilianum* f. sp. *zeae*, 1,744 unique GO terms could be  
295 assigned to 4,124 proteins in *S. reilianum* f. sp. *reilianum* and 1,757 unique GO terms could  
296 be assigned to 3,922 proteins in *U. hordei* (supplementary table S3). The Bioconductor  
297 package topGO (Alexa et al. 2006) was then used to link each GO term to the three major  
298 categories “Cellular Component”, “Biological Process” or “Molecular Function”. Enrichment  
299 analysis was performed by computing *P* values for each GO term using Fisher’s classic test  
300 with parent-child correction (Grossmann et al. 2007). Cytoplasmic proteins with and without  
301 signatures of positive selection were compared for the three species separately, and  
302 differences were considered to be significant at the 5 % level.

303

#### 304 *Strains and growth conditions*

305 The *Escherichia coli* derivative Top10 (Invitrogen, Karlsruhe, Germany) and the  
306 *Saccharomyces cerevisiae* strain BY4741 (*MATa his3Δ1 leu2Δ met15Δ ura3Δ*; Euroscarf,  
307 Frankfurt, Germany; kindly provided by M. Bölker, Marburg) were used for cloning  
308 purposes. *Sporisorium reilianum* strains used in this study are listed in supplementary table 4.  
309 They are derivatives of the haploid solopathogenic strain JS161 which is capable of plant  
310 colonization without the need of a mating partner, because it expresses a compatible  
311 pheromone/receptor pair (Schirawski et al. 2010). *Escherichia coli* was grown in dYT liquid  
312 medium (1.6 % (w/v) Trypton, 1.0 % (w/v) Yeast Extract (Difco), 0.5 % (w/v) NaCl) or YT  
313 solid medium (0.8 % (w/v) Trypton, 0.5 % (w/v) Yeast-Extract, 0.5 % (w/v) NaCl, 1.3 %  
314 (w/v) agar) supplemented with 100 mg/mL Ampicillin when needed. The yeast *S. cerevisiae*  
315 was maintained in YPD solid medium (1 % (w/v) yeast extract, 2 % (w/v) Bacto-Peptone, 2 %  
316 (w/v) Bacto-Agar, 2 % (w/v) glucose) and grown on SC URA<sup>-</sup> medium (1.7 % (w/v) Yeast  
317 Nitrogen Base without ammonium sulfate, 0.147 % (w/v) dropout-mix without Uracil, 2 %  
318 (w/v) glucose) for selecting transformants containing the plasmid pRS426 (Sikorski and

319 Hieter 1989) (kindly provided by M. Bölker, Marburg) or derivatives of pRS426. Strains of *S.*  
320 *reilianum* were grown in liquid YEPS<sub>light</sub> medium (1.0 % (w/v) yeast extract, 0.4% (w/v)  
321 peptone, 0.4% (w/v) sucrose) at 28°C on a rotary shaker at 200 rpm.

322

### 323 *Construction of S. reilianum strains*

324 Polymerase chain reactions were performed using the Phusion High-Fidelity DNA  
325 Polymerase (New England Biolabs). Templates were either JS161 genomic or indicated  
326 plasmid DNA. Restriction enzymes were obtained from New England Biolabs. Protoplast-  
327 mediated transformation was used to transform *S. reilianum* following a method established  
328 for *U. maydis* (Schulz *et al.* 1990). Transformants were selected on RegAgar plates (1.0 %  
329 (w/v) yeast extract, 0.4 % (w/v) Bacto-Peptone, 0.4 % (w/v) Sucrose, 1 M Sorbitol, 1.5 %  
330 (w/v) Bactoagar) supplemented with 200 µg/mL Geneticin and true resistance was tested by  
331 growing single colonies on PD plates (3.9 % (w/v) Potato-Dextrose Agar, 1 % (v/v) Tris-HCl  
332 (1M, pH 8.0)) supplemented with 50 µg/mL Geneticin. Gene replacements with resistance  
333 markers were generated with a PCR-based method employing the previously described *Sfi*I  
334 insertion cassette system (Brachmann *et al.* 2004; Kämper 2004) and were confirmed by  
335 Southern blot analysis. Genomic regions residing about 1 kb upstream (left border) or  
336 downstream (right border) adjacent to open reading frames of candidate genes were PCR-  
337 amplified using the listed primer pairs (supplementary table S5) and genomic DNA of JS161  
338 as template. The resulting fragments were used for cloning plasmids containing the respective  
339 deletion constructs.

340 To obtain deletion constructs for the genes *sr10529* and *sr14347*, PCR fragments containing  
341 the left and right borders of each gene were ligated to the hygromycin resistance cassette of  
342 pBS-hhn (Kämper 2004) via *Sfi*I restriction sites and cloned into pCRII-TOPO (Life  
343 Technologies) to generate pTOPO Δ*sr10529* #1 and pTOPO Δ*sr14347* #1, respectively. Since

344 the use of Geneticin as selection marker resulted in much less false positive transformants  
345 compared to the use of Hygromycin B, the hygromycin resistance cassettes in these plasmids  
346 were replaced by the Geneticin resistance cassette of pUMA 1057 (Brachmann et al. 2004) by  
347 ligation via *Sfi*I restriction sites, yielding plasmids pTOPO  $\Delta$ sr10529 G418 and pTOPO  
348  $\Delta$ sr14347 Gen #1, respectively. Deletion constructs were PCR-amplified from plasmids  
349 pTOPO  $\Delta$ sr10529 G418 and pTOPO  $\Delta$ sr14347 Gen #1 using the listed primers  
350 (supplementary table S5) and used to transform the *S. reilianum* strain JS161 to generate the  
351 gene deletion strains JS161 $\Delta$ sr10529 and JS161 $\Delta$ sr14347, respectively.

352 The drag and drop cloning method in yeast (Jansen et al. 2005) was used to generate plasmids  
353 pRS426  $\Delta$ sr12968 Hyg #1, pRS426  $\Delta$ sr14944 Hyg #2, pRS426  $\Delta$ sr10059 Hyg #1, pRS426  
354  $\Delta$ sr10182 Hyg #1, pRS426  $\Delta$ sr14558 Hyg #1 and pRS426  $\Delta$ sr12897 Hyg #1 which contain  
355 deletion constructs for deleting the candidate genes *sr12968*, *sr14944*, *sr10059*, *sr10182*,  
356 *sr14558* or *sr12897*. These plasmids are a derivate of plasmid pRS426, which can be  
357 maintained in *E. coli* and *S. cerevisiae* (Sikorski and Hieter 1989). PCR-amplified left and  
358 right borders of each candidate gene and the hygromycin resistance cassette were integrated in  
359 pRS426 by homologous recombination in *S. cerevisiae*. Subsequently, the hygromycin  
360 resistance cassette was replaced with the Geneticin resistance cassette by ligation via *Sfi*I  
361 restriction sites, yielding plasmids pRS426  $\Delta$ sr12968 Gen #1, pRS426  $\Delta$ sr14944 Gen #3,  
362 pRS426  $\Delta$ sr10059 Gen #1, pRS426  $\Delta$ sr10182 Gen #1, pRS426  $\Delta$ sr14558 Gen #1 and pRS426  
363  $\Delta$ sr12897 Gen #5, respectively. Gene deletion constructs were PCR-amplified from the  
364 respective plasmid using listed primers (supplementary table S5). The obtained deletion  
365 constructs were used to transform the *S. reilianum* strain JS161 to generate the gene deletion  
366 strains JS161 $\Delta$ sr12968, JS161 $\Delta$ sr14944, JS161 $\Delta$ sr10059, JS161 $\Delta$ sr10182, JS161 $\Delta$ sr14558  
367 and JS161 $\Delta$ sr12897, respectively.

368 The drag and drop cloning method was also used to generate plasmid pRS426  $\Delta$ sr12084 Gen  
369 #1. PCR-amplified left and right borders of *sr12084* and the Geneticin resistance cassette were  
370 integrated in pRS426 by homologous recombination in *S. cerevisiae*. The gene deletion  
371 construct for deleting the candidate gene *sr12084* was PCR-amplified from plasmid pRS426  
372  $\Delta$ sr12084 Gen #1 using primers sr12084\_lb\_fw/sr12084\_rb\_rv and transformed into the *S.*  
373 *reilianum* strain JS161 to generate the gene deletion strain JS161 $\Delta$ sr12084.

374

375

376

377 *Virulence assays*

378 The solopathogenic strain JS161 and derivatives thereof were grown in YEPS<sub>light</sub> liquid  
379 medium to an optical density at 600 nm (OD<sub>600</sub>) of 0.8 - 1.0 and cell cultures were adjusted to  
380 an OD<sub>600</sub> of 1.0 with sterile water prior to injection into one-week old maize (*Zea mays*)  
381 seedlings of the dwarf cultivar ‘Gaspé Flint’ (kindly provided by B. Burr, Brookhaven  
382 National Laboratories and maintained by self-pollination). Plants were sowed in T-type soil of  
383 ‘Fruhstorfer Pikiererde’ (HAWITA, Vechta, Germany) and grown in a temperature-controlled  
384 greenhouse (14h-/10h- light/dark cycle, with 28/20°C and 25,000 – 90,000 lux during the  
385 light period). Virulence symptoms were scored nine to ten weeks post infection according to  
386 previously described symptoms (Ghareeb et al. 2011) and the following categories were  
387 distinguished: the plant did not develop ears, the plant developed healthy ears shorter or equal  
388 to 1 cm or the plant developed healthy ears longer than 1 cm, the plant developed spiky ears,  
389 phyllody in ears or phyllody in tassels. Spore formation was only observed occasionally, and  
390 rarely the plant died due to the infection. Three independent infections were carried out per  
391 strain, mock treated plants were infected with water as control and at least three independent  
392 deletion strains were tested for virulence.

393

394

## 395 **Results**

396 *Candidate effector genes are less conserved between species compared to other genes*

397 We reconstructed families of homologous genes for the five smut fungi *U. hordei*, *U. maydis*,  
398 *S. scitamineum*, *S. reilianum* f. sp. *zeari* and *S. reilianum* f. sp. *reilianum* using the SiLiX  
399 clustering algorithm (Miele et al. 2011). We optimized the clustering parameters to maximize  
400 the occurrence of orthologues and minimize the number of paralogues within each family. In  
401 this way, we were able to reconstruct 8,761 families, among which 5,266 had at least one  
402 gene in each species (supplementary table S6). As a consequence, we found at least one  
403 homologous sequence in four species for 78 % of all genes. 5,254 gene families are found to  
404 have exactly one member in each species and were therefore taken as true orthologues  
405 (referred to as “core orthologous set” in the following). Considering that secreted proteins are  
406 putative effectors, we used SignalP (Petersen et al. 2011) to predict secretion of the encoded  
407 protein for each gene (supplementary table S1). We report that 920 (11 %) families contained  
408 only genes encoding a predicted secreted protein, while 7,657 (87 %) contained only genes  
409 encoding a protein not predicted to be secreted. The remaining 184 (2 %) families contained  
410 both predicted secreted and cytoplasmic proteins (supplementary table S6). The occurrence of  
411 families with both secreted and cytoplasmic proteins can be explained by (1) false negative  
412 predictions for secretion, as truncated C-terminal sequences were not removed from the data  
413 set, (2) wrong gene annotations or (3) gain or loss of a secretion signal peptide during effector  
414 evolution (Poppe et al. 2015). Among all predicted secreted proteins, 52 % have at least one  
415 orthologue in all other species, which is significantly less than the global 78 % proportion for  
416 all proteins (Chi-squared test,  $P$  value  $< 2.2 \times 10^{-16}$ ). Genes encoding putative effector proteins  
417 are therefore less conserved across species than other genes, either because their sequence is



418 evolving faster, preventing the recovery of homologous relationships, or because effector  
419 genes are created or lost at a higher rate. In *U. hordei*, we observe several species-specific  
420 family expansions. There were 17 families which encompassed five to 25 members, but no  
421 orthologue in other species (supplementary table S6). Moreover, we identified three families  
422 with up to 62 members in *U. hordei*, but only one member in up to three of the other species  
423 (supplementary table S6). Gene duplications in *U. hordei* have been hypothesized to be driven  
424 by mobile elements (Laurie et al. 2012).

425

426 *The genomes of S. reilianum f. sp. zae and S. reilianum f. sp. reilianum diverged around one*  
427 *million years ago*

428 To establish a frame for our comparative analysis we first calculated sequence similarity of  
429 the five smut fungi for non-coding intergenic and protein sequences. In addition, we estimated  
430 divergence times by performing a molecular dating analysis based on the core orthologues set  
431 of the five pathogens, using advanced models of protein sequence evolution and Bayesian  
432 inference as implemented in the PhyloBayes package (Lartillot et al. 2009). As calibration  
433 point, we used the divergence time of *U. hordei* and *U. maydis*, previously estimated to be  
434 between 27 and 21 Myr (Bakkeren and Kronstad, 2007). In alignable intergenic regions *U.*  
435 *hordei* shares 57 % identity with *S. reilianum f. sp. reilianum* and 77 % identity in protein  
436 sequences (fig. 1B). Monte-Carlo Markov chains were run for three independent gene  
437 samples totaling more than 20,000 amino acid positions each, and two chains were run in  
438 each case to assess convergence. The resulting posterior distribution of divergence times were  
439 used to infer 95 % posterior intervals. The split between *U. maydis* and the *Sporisorium*  
440 species was estimated to have occurred around 20 Myr ago (95 % posterior interval 25 to 12  
441 Myr; fig 1A and supplementary table S2). *Sporisorium reilianum f. sp. reilianum* shares 61 %  
442 nucleotide identity in alignable intergenic regions with *U. maydis*, and 79 % sequence identity

443 at the protein level (fig. 1B). The divergence times of *S. scitamineum* and the two formae  
444 speciales of *S. reilianum* were calculated to be 13 Myr ago (95 % posterior interval 19 to 7  
445 Myr; fig. 1A and supplementary table S2), which is consistent with the mean divergence  
446 estimated between the hosts sorghum and sugarcane (10 Myr with a posterior interval of 8 to  
447 13 Myr, average over eight studies, source: timetree.org (Kumar et al. 2017)). *Sporisorium*  
448 *reilianum* f. sp. *reilianum* and *S. scitamineum* share 74 % non-coding nucleotide identity and  
449 88 % identity at the protein level (fig. 1B). Finally, the two *S. reilianum* strains diverged 1.1  
450 Myr ago (95 % posterior interval 2.4 to 0.4 Myr; fig. 1A) and share 98 % noncoding  
451 nucleotide identity and 99 % protein identity (fig. 1B). We note that the estimation of this  
452 divergence date varied with the gene set used, and was in some cases found to be older (1.7  
453 Myr, with a 95 % posterior interval of 4.7 to 0.6 Myr, see supplementary table S2). The  
454 comparison of the five smut genomes therefore encompasses a broad evolutionary time, and  
455 the divergence times obtained are compatible with previous estimates from smaller data sets  
456 (Munkacsi et al., 2007). The speciation times of the investigated smut species largely predate  
457 the 10,000 years of crop plant domestication, which implies that adaptation to the agricultural  
458 host, if any, will be negligible when interpreting the inter-specific patterns of sequence  
459 divergence, as it represents a marginal proportion of the time since the divergence from the  
460 ancestral species.

461

462 *Sporisorium reilianum* contains the largest number of positively selected genes

463 To detect positive selection, 6,205 families with at least three members (orthologues and/or  
464 paralogues, see supplementary table S6) were, regardless of their species composition, aligned  
465 on the codon and amino acid level and a phylogenetic tree was inferred. Obtaining accurate  
466 alignments is critical for detecting positive selection since alignment errors frequently inflate  
467 the false discovery rate (Schneider et al. 2009; Jordan and Goldman 2012). We therefore

468 developed a stringent bioinformatics pipeline for the filtering of sequence alignments by  
469 masking ambiguous alignment positions for further analysis (see Methods). To scan for  
470 positive selection, we employed a non-homogeneous model of sequence evolution allowing  
471  $d_N/d_S$  ratios to vary along the phylogeny, in combination with two heuristic model selection  
472 procedures to avoid over-parametrization issues (Nielsen and Yang 1998; Dutheil et al. 2012).  
473 Model parameters could not be fitted by either one of the two methods in 1.7% of branches.  
474 The two model selection procedures led to highly consistent estimates of branch-specific  $d_N /$   
475  $d_S$  ratios (Spearman's rank correlation coefficient equal to 0.85,  $p$ -value  $< 2.2 \times 10^{-16}$ ). The  
476 distribution of  $d_N / d_S$  was highly skewed with a median value of 0.06, demonstrating the  
477 strong predominance of purifying selection throughout lineages and genes. The mean value of  
478  $d_N / d_S$  ratios for lineages undergoing positive selection ( $d_N / d_S > 1$ ) was 4.1 (median 1.9).  
479 While a  $d_N / d_S$  ratio above one is indicative of positive selection, the absolute value of the  
480 ratio is a poor indicator of the strength of undergoing selection. In particular, high ratio values  
481 can be obtained because of low  $d_S$  values, and the  $d_N$  rate might include neutral substitutions,  
482 such as non-synonymous substitution that are conservative regarding certain biochemical  
483 properties of the amino-acids involved (Sainudiin et al. 2005). The largest number of genes  
484 with signs of positive selection was found in *S. reilianum* f. sp. *zeae* (84 genes, of which 25  
485 encode predicted secreted proteins) and *S. reilianum* f. sp. *reilianum* (111 genes of which 27  
486 encode predicted secreted proteins) (fig. 1C). In addition, a substantial number of positively  
487 selected candidate genes was also found in *U. hordei* (49, and of these, 22 genes are predicted  
488 to code for secreted proteins), but only very few in *U. maydis* (2 genes) and *S. scitamineum* (7  
489 genes) (fig. 1C). A list of all proteins with their associated  $d_N/d_S$  ratios in each species is  
490 provided in supplementary table S3. Predicted secreted proteins were significantly enriched in  
491 the group of proteins under positive selection in *U. hordei* and in the two investigated formae  
492 speciales of *S. reilianum* ( $P$  values  $< 10^{-5}$ ; Fisher's exact test). This corroborates results of

493 earlier studies in other pathosystems that showed that predicted secreted proteins are often  
494 under positive selection, which can be attributed to their direct interaction with host proteins  
495 (Joly et al., 2010; Wicker et al. 2013; Poppe et al., 2015). Notably, all genes found under  
496 positive selection in the two strains of *S. reilianum*, in *S. scitamineum* and in *U. maydis* share  
497 orthologous genes in the other species (supplementary tables S3 and S6). In contrast, genes  
498 with signs of positive selection in *U. hordei* belong largely (36 out of 49 genes) to families  
499 showing species-specific expansions (supplementary tables S3 and S6).

500

501 *Genes under positive selection in U. hordei are associated with uncharacterized interspersed*  
502 *repeats*

503 Among the species compared here, the genome of *U. hordei* shows the highest fraction of  
504 repetitive elements (Laurie et al. 2012; Dutheil et al. 2016). Such elements are known to  
505 contribute to gene family expansions (Kazazian 2004), and have been suggested to contribute  
506 to adaptation by providing advantageous mutations, for instance by repeat-induced point  
507 mutations (RIP) leakage which was revealed in a species complex of *Leptosphaeria* (Rouxel  
508 et al. 2011; Grandaubert et al., 2014). As sequence signatures of RIP were found in LTR  
509 elements of *U. hordei* (Laurie et al., 2012), we tested whether genes under positive selection  
510 in *U. hordei* are physically associated with repetitive elements. We performed a binary  
511 logistic regression with the prediction of positive selection as a response variable (that is,  
512 whether the underlying branch has a  $d_N/d_S$  ratio higher than one) and we considered three  
513 putative explanatory variables for each analyzed gene: (1) whether the gene is predicted to  
514 encode a secreted protein, (2) whether the gene is duplicated and (3) the distance of the gene  
515 to the closest interspersed repeat. The complete linear model explains 50 % of the observed  
516 variance, and the three explanatory variables are all significant at the 0.1 % level  
517 (supplementary table S7). These results suggest that positively selected genes in *U. hordei* are

518 associated with duplication events, and positive selection is more likely to occur at genes  
519 encoding putative effectors. In addition, the proximity of interspersed repeats increases the  
520 odds of positive selection, independently of the two other effects, and is confirmed by a  
521 stratification approach: the effect still holds when only duplicated genes are considered, or  
522 only genes encoding a secreted protein, or the combination of the two (supplementary table  
523 S7). This finding corroborates previous results obtained in other microbial plant pathogens  
524 where it was described that effector genes tend to localize in repeat rich regions and where it  
525 was suggested that such regions contribute to the rapid evolution of effector genes (Raffaele  
526 and Kamoun, 2012).

527 *Positively selected genes encoding cytoplasmic proteins in S. reilianum and U. hordei*

528 While we expect effector genes to be under positive selection, we find that the majority of  
529 positively selected genes in *S. reilianum* encodes cytoplasmic proteins (fig. 1C). To assess the  
530 putative functional role of these genes, we performed a Gene Ontology term enrichment  
531 analysis, comparing cytoplasmic proteins under positive selection to cytoplasmic proteins not  
532 under positive selection (table 1). This analysis revealed that genes with a potential role in  
533 metabolic processes, like sulfur compound metabolism, molybdopterin cofactor metabolic  
534 process, RNA metabolic process, organic cyclic compound metabolic process and  
535 oxidoreductase activity, as well as responses to starvation and extracellular stimuli are  
536 significantly overrepresented at the 5% level (Fisher's classic test with Parent-Child  
537 correction; see table 1). This could indicate that cytoplasmic proteins under positive selection  
538 contribute to metabolic changes which might be needed to survive with the limited nutrients  
539 available on the surface or in the biotrophic interface of different host plants. A similar  
540 analysis for cytoplasmic proteins under positive selection in *U. hordei* was conducted, but  
541 only led to top-level categories (DNA integration, DNA metabolic process and isomerase  
542 activity; see table 1).

543

544 *Virulence contribution of effector genes showing signs of positive selection in S. reilianum*

545 Candidate effector genes inferred to be under positive selection in a particular species could  
546 play a critical role in pathogenicity. Therefore, we sought to assess the contribution to  
547 virulence of such candidate genes by creating individual deletion mutants. In total, we tested  
548 nine candidate genes with high  $d_N/d_S$  ratios and predicted to encode secreted proteins: three  
549 with signatures of positive selection only in *S. reilianum* f. sp. *zeae*, three with signatures of  
550 positive selection in *S. reilianum* f. sp. *zeae* as well as in *S. reilianum* f. sp. *reilianum* and  
551 three with signatures of positive selection only in *S. reilianum* f. sp. *reilianum*. All nine  
552 chosen candidate genes together with their characteristics are summarized in table 2. Deletion  
553 mutants were generated in the haploid solopathogenic strain JS161 of *S. reilianum* f. sp. *zeae*.  
554 This strain is capable of colonizing maize plants and cause disease without a compatible  
555 mating partner (Schirawski et al. 2010) but virulence is much reduced relative to infection  
556 with mating-compatible wild-type strains and spores are only rarely produced. Deletion  
557 mutants were also generated in strain JS161 in cases where positive selection was only  
558 detected in *S. reilianum* f. sp. *reilianum* (table 2), because no solopathogenic strain is  
559 presently available for *S. reilianum* f. sp. *reilianum*. For each gene at least three independent  
560 deletion mutants were generated and tested for virulence. To determine virulence, Gaspe  
561 Flint, a dwarf variety of corn, was infected and symptoms were scored in male and female  
562 flowers (fig. 2). Only the deletion of *sr10529*, a gene showing positive selection in both  
563 formae speciales of *S. reilianum*, showed a strong reduction in virulence (table 2 and fig. 2).  
564 The gene *sr10529* in *S. reilianum* f. sp. *zeae* is orthologous to the previously identified and  
565 characterized gene *pit2* (*UMAG\_01375*) in *U. maydis*.  
566 *Pit2* plays an essential role in virulence as inhibitor of a group of maize papain-like cysteine  
567 proteases that are secreted to the apoplast (Doehlemann et al. 2011; Mueller et al. 2013).

568 Previous work identified a conserved domain of 14 amino acids (PID14) in Pit2 as required  
569 and sufficient for the inhibition of maize cysteine proteases (Mueller et al. 2013). When the  
570 branch-site model of PAML 4 (Yang 2007) was used to identify amino acid residues under  
571 positive selection in the Pit2 orthologues of the two *S. reilianum* species, only two residues  
572 residing in the PID14 domain were found under positive selection. However, 24 positively  
573 selected residues were detected outside this domain in the 57 amino acid long C-terminal part  
574 (fig. 3).

575

576

577

578

## 579 **Discussion**

580 We used evolutionary comparative genomics of five related smut fungi infecting four  
581 different host plants to identify genes with a signature of positive selection during species  
582 divergence, with a focus on genes encoding predicted secreted proteins, as such genes were  
583 suggested to contribute to virulence in various plant pathogenic microbes (Aguileta et al.  
584 2010; Stukenbrock et al. 2011; Hacquard et al. 2012; Dong et al. 2014; Huang et al. 2014;  
585 Sharma et al. 2014). Our analysis revealed that positive selection is found between paralogous  
586 genes in *U. hordei*, where they belong to families with species-specific expansions. In  
587 contrast, genes under positive selection in the other four species belong to families of  
588 orthologous sequences. While we find evidence for a large set of genes under positive  
589 selection in the *S. reilianum* species, signatures for positive selection are hardly detectable in  
590 the more distant relatives *U. hordei*, *U. maydis* and *S. scitamineum* that diverged earlier.  
591 Finding evidence for positive selection over time spans of several millions of years is  
592 notoriously difficult (Gillespie 1994) because of two main reasons: (1) periods where genes

593 are evolving under positive selection may occur episodically and may be followed by long  
594 episodes of purifying selection, leading to an average  $d_N/d_S$  below 1 on long periods of time  
595 and (2) fast evolving genes may diverge to an extent where their homology is difficult to infer  
596 and where they can no longer be aligned reliably. To overcome this problem, more genome  
597 information of species with intermediate branching points is needed (Gillespie 1994).

598 Predicted secreted proteins were about three times overrepresented in the set of positively  
599 selected genes, which illustrates the importance of secreted proteins in adaptation processes of  
600 smut fungi. This also corroborates results in other plant pathogenic microbes like *Melampsora*  
601 *sp.*, *Z. tritici* and the wheat powdery mildew *Blumeria graminis* (Joly et al. 2010; Stukenbrock  
602 et al. 2011; Wicker et al. 2013). However, the majority of positively selected genes encodes  
603 cytoplasmic proteins (fig. 1C), suggesting that both secreted and non-secreted proteins are  
604 important targets of adaptation. A Gene Ontology analysis in *S. reilianum* showed that mainly  
605 processes related to metabolism and its regulation as well as responses to starvation and  
606 external stimuli are enriched in cytoplasmic proteins under positive selection. This points at a  
607 role of these proteins in adaptation to differences in nutrient availability in the respective host  
608 plants maize and sorghum as well as responses to cues originating from the respective host  
609 (Haeuelsen and Stukenbrock 2016). A study conducted in *U. maydis* has shown that the fungus  
610 induces major metabolic changes in the host plant upon infection during establishment of  
611 biotrophy and undergoes a series of developmental transitions during host colonization that  
612 are likely influenced by the host environment (Doehlemann et al. 2008). It is thus conceivable  
613 that the two *S. reilianum* accessions have adapted to their different hosts that differ  
614 significantly for example in their amino acid and vitamin composition (Etuk et al. 2012).  
615 Furthermore, recent studies in *U. maydis* suggested that intracellular changes of metabolism  
616 influence virulence, and therefore the underlying proteins could be targets of positive  
617 selection (Kretschmer et al. 2012; Goulet et al. 2017).



618 Out of nine deletions of positively selected genes, only one mutant, lacking *sr10529*, was  
619 affected in virulence. While six of the deleted genes are single genes in *S. reilianum* f. sp.  
620 *zea* for which we failed to identify paralogs, *sr12084* has two paralogs, *sr14347* has five  
621 paralogs and *sr10182* has ten paralogs. We restricted our analyses to generating deletion  
622 mutants in some of the genes under positive selection. This leaves open the possibility that the  
623 paralogous genes have redundant functions in virulence. Adapting the CRISPR-Cas9  
624 technology allowing multiplexing (Schuster et al. 2017) to *S. reilianum* will be instrumental  
625 in testing this hypothesis in future studies. Alternatively, the candidate effectors we  
626 investigated may be needed under conditions which differ from those tested here. For  
627 example, *S. reilianum* f. sp. *zea* can also systemically colonize maize plants via root  
628 infection (Mazaheri-Naeini et al. 2015), a colonization route we have not assessed in our  
629 experimental setup. Moreover, we employed only one maize cultivar for infection assays.  
630 Results from other pathosystems suggest that virulence effects can strongly depend on the  
631 host and pathogen genotypes, in particular in the presence of *R* and *avr* genes (Petit-Houdenot  
632 and Fudal, 2017). No *avr-R* gene interaction was described so far in the *S. reilianum* f. sp.  
633 *zea*-maize pathosystem. Instead, quantitative virulence differences are observed when  
634 different host cultivars are infected (Lübberstedt et al. 1999). Knowing the expression profile  
635 of effector genes may assist the identification of differences in development of the mutants  
636 compared to wild type strains. Since we lack this information, we scored disease symptoms  
637 only in the inflorescences about nine weeks after infection. Additionally, it may be possible  
638 that small differences in virulence between JS161 and deletion mutants of candidate genes  
639 remain undetected due to the weak infection behavior of JS161. For example, spore formation  
640 is only rarely observed after infecting maize plants with the solopathogenic strain. In contrast,  
641 infections resulting from infections with two compatible haploid strains show spores in about  
642 40 % of the infected plants (Zuther et al. 2012). This means that defects related to spore

643 formation will not be evident in mutants of JS161. In three cases positive selection was  
644 detected in orthologous genes in *S. reilianum* f. sp. *reilianum* while candidate effector genes  
645 were for experimental reasons deleted in *S. reilianum* f. sp. *zeae*. Therefore, it cannot be  
646 excluded that these effectors might have a virulence function in *S. reilianum* f. sp. *reilianum*.  
647 In this case, the positively selected effector genes might have evolved during adaptation to the  
648 sorghum host and present host specificity genes. In summary, our virulence assays leave open  
649 the possibility that the eight candidate genes which did not show a contribution to virulence  
650 could play a role in pathogenicity under conditions not tested here. Alternatively, candidate  
651 effector proteins might also be positively selected for traits that are not directly linked to  
652 pathogenicity. Such traits could for instance involve competition with large numbers of other  
653 plant colonizing microbes (Zhan and McDonald 2013; Rovenich et al. 2014). Secreted  
654 proteins of *S. reilianum* could act for example as toxin or could efficiently utilize resources  
655 from the environment and thereby limit the growth of other microbes. In these cases, a  
656 contribution to virulence is not expected to be observed in the employed infection assay with  
657 the effector gene mutants. Moreover, our molecular dating analysis showed that the common  
658 ancestors of the investigated smut species originated before the beginning of crop  
659 domestication. Therefore, positive selection, whose signs we detect by our approach, has most  
660 likely occurred on ancestral host plants and not on the domesticated host maize.  
661 Consequently, some of the candidate effector genes under positive selection might not be  
662 important for the colonization of crop plants, but for infection of related wild species.  
663 In *U. maydis*, we note that effector genes residing in clusters whose deletion affected  
664 virulence (Kämper et al. 2006; Schirawski et al. 2010) have similar  $d_N/d_S$  ratios as effector  
665 genes in clusters where the deletion had no effect on virulence (median  $d_N/d_S$  ratio 0.0619  
666 vs. 0.1094; Wilcoxon rank test with  $P$  value = 0.1848). Furthermore, orthologues of the  
667 effectors Pep1, Stp1 and Cmu1, which were shown to have important roles in pathogenicity of

668 *U. maydis* (Djamei et al. 2011; Doehlemann et al. 2009; Schipper 2009) showed no signature  
669 of positive selection. These observations could suggest that certain fungal effector proteins  
670 are under evolutionary constraint and are therefore not free to accumulate non-synonymous  
671 mutations. Such effectors are conserved over long time spans (Schirawski et al. 2010;  
672 Hemetsberger et al. 2015; Sharma et al. 2015) and this illustrates that they are instrumental  
673 for successful infections in a large group of smut fungi. They probably target molecules  
674 shared by several host plants, for example housekeeping functions that cannot easily evolve in  
675 response to the binding of an effector.

676 One candidate gene (*sr10529*) under positive selection in both formae speciales of *S.*  
677 *reilianum* showed a strong contribution to virulence upon deletion. It is orthologous to the  
678 previously described protease inhibitor Pit2 in *U. maydis*, where the deletion also abolished  
679 virulence (Doehlemann et al. 2011; Mueller et al. 2013). Positively selected residues in the  
680 PID14 domain of Pit2 might reflect that different proteases need to be inhibited in maize and  
681 sorghum. Pit2 might thus contribute to determining the host range of the respective species. A  
682 role of cysteine protease inhibitors in host specificity was demonstrated in *Phytophthora*  
683 *infestans*, a pathogen of potato and its sister species *Phytophthora mirabilis*, which infects the  
684 ornamental plant *Mirabilis jalapa*. Positively selected orthologous protease inhibitors were  
685 shown to inhibit proteases specific to the respective host plants and this specificity could be  
686 traced back to a single amino acid substitution (Dong et al. 2014). Surprisingly, 24 positively  
687 selected sites in Pit2 were detected outside the PID14 domain in the 57 amino acid long C-  
688 terminal part in both *S. reilianum* f. sp. *zea* and *S. reilianum* f. sp. *reilianum*. This finding  
689 raises the intriguing possibility that the C-terminus of Pit2 might possess a second function  
690 that is independent of protease inhibition. Earlier work has shown that the *pit1* gene encoding  
691 a transmembrane protein is located next to the *pit2* effector gene and both genes contribute  
692 similarly to virulence (Doehlemann et al. 2011). Furthermore, *pit1* and *pit2* are divergently

693 transcribed, which makes it likely that the expression of *pit1* and *pit2* is co-regulated. In  
694 addition, this gene arrangement of *pit1* and *pit2* is conserved in *U. hordei*, *U. maydis*, *S.*  
695 *scitamineum* and *S. reilianum* (Sharma et al. 2015). This finding has led to the speculation  
696 that Pit1 and Pit2 somehow act together to govern virulence of *U. maydis* and related smut  
697 fungi. It was hypothesized that that Pit2 shuttles apoplastic maize proteins towards Pit1,  
698 thereby scavenging damage-associated molecules (Doehlemann et al. 2011). In this scenario,  
699 the positively selected amino acids in the C-terminus of Pit2 could have been selected for  
700 scavenging such molecules as adaptation to the two hosts. In future studies it will be highly  
701 interesting to complement the *pit2* mutant of *S. reilianum* f. sp. *zeae* with the *pit2* orthologue  
702 of *S. reilianum* f. sp. *reilianum* to see if this promotes virulence on sorghum.

703

704

## 705 **Conclusions**

706 Screens for genes with signs of positive selection are commonly used to identify candidate  
707 effector genes in various plant pathogenic microbes. However, it is currently largely open  
708 whether positively selected effector genes play indeed a role in virulence. Here, we used  
709 comparative genomics of five smut fungi and showed that only one out of nine genes under  
710 positive selection contributes to virulence of *S. reilianum*. Moreover, the majority of  
711 positively selected genes did not encode predicted secreted proteins. Our results leave open  
712 the possibility that many genes with signatures of positive selection contribute to virulence  
713 under conditions not tested in this study or are selected in traits that are not directly related to  
714 pathogenicity.

715

716

## 717 **Acknowledgements**

718 Our work was supported through the LOEWE program of the state of Hesse through  
719 SYNMICRO and through the Max Planck Society. GS was funded by the International Max  
720 Planck Research School (IMPRS) for Molecular, Cellular and Environmental Microbiology.  
721 We thank Michael Bölker for providing the yeast strain BY4741 and the plasmid pRS426  
722 which were used for cloning purposes, and Benoit Nabholz and Nicolas Lartillot for guidance  
723 with the dating analysis. We are grateful to Markus Rampp (Max Planck Computing Center  
724 Garching) for assistance with computational work and to Stefan Schmidt for expert  
725 greenhouse service, as well as all present and former group members for lively discussions  
726 and Eva H. Stukenbrock for her comments on the manuscript.

727

728

729

## 730 **References**

- 731 Anikster Y. 1984. The *Formae Speciales*. In: Bushnell WR and Roelfs AP (Eds.) *The cereal*  
732 *rusts*. Academic Press (London).
- 733 Aguileta G, et al. 2012. Genes under positive selection in a model plant pathogenic fungus,  
734 *Botrytis*. *Infect Genet Evol* 12: 987-996.
- 735 Aguileta G, et al. 2010. Finding candidate genes under positive selection in non-model  
736 species: examples of genes involved in host specialization in pathogens. *Mol Ecol* 19: 292-  
737 306.
- 738 Aguileta G, Refregier G, Yockteng R, Fournier E, Giraud T. 2009. Rapidly evolving genes in  
739 pathogens: methods for detecting positive selection and examples among fungi, bacteria,  
740 viruses and protists. *Infect Genet Evol* 9: 656-670.
- 741 Alexa A, Rahnenführer J, Lengauer T. 2006. Improved scoring of functional groups from  
742 gene expression data by decorrelating GO graph structure. *Bioinformatics* 22: 1600-1607.
- 743 Altschul SF, Gish W, Miller W, Myers EW, Lipman DJ. 1990. Basic local alignment search  
744 tool. *J Mol Biol* 215: 403-410.

- 745 Bagchi R, et al. 2014. Pathogens and insect herbivores drive rainforest plant diversity and  
746 composition. *Nature* 506: 85-88.
- 747 Bakkeren G, Kronstad JW. 2007. Bipolar and Tetrapolar Mating Systems in the Ustilaginales.  
748 In: Heitman J, Kronstad JW, Taylor J, Casselton L (eds). *Sex in fungi*. ASM Press,  
749 Washington.
- 750 Begerow D, et al. 2014. Ustilaginomycotina. In: Esser K (ed). *The Mycota - A comprehensive*  
751 *treatise on fungi as experimental systems for basic and applied research. Systematics and*  
752 *evolution (Part A)*. Springer, Heidelberg.
- 753 Blanchette M, et al. 2004. Aligning multiple genomic sequences with the Threaded Blockset  
754 Aligner. *Genome Res* 14: 708-715.
- 755 Brachmann A, König J, Julius C, Feldbrügge M. 2004. A reverse genetic approach for  
756 generating gene replacement mutants in *Ustilago maydis*. *Mol Genet Genomics* 272: 216-226.
- 757 Brown JKM, Tellier A. 2011. Plant-parasite coevolution: bridging the gap between genetics  
758 and ecology. *Annu Rev Phytopathol* 49: 345-367.
- 759 Charif D, Lobry JR. 2007. SeqinR 1.0-2: a contributed package to the R project for statistical  
760 computing devoted to biological sequences retrieval and analysis. In: Bastolla U, Porto M,  
761 Roman HE, Vendruscolo M, editors. *Structural approaches to sequence evolution: Molecules,*  
762 *networks, populations*. New York: Springer Verlag. p. 207-232.
- 763 Dean R, et al. 2012. The top 10 fungal pathogens in molecular plant pathology. *Mol Plant*  
764 *Pathol* 13: 414-430.
- 765 de Jonge R, Bolton MD, Thomma BP. 2011. How filamentous pathogens co-opt plants: the  
766 ins and outs of fungal effectors. *Curr Opin Plant Biol* 14: 400-406.
- 767 Djamei A, et al. 2011. Metabolic priming by a secreted fungal effector. *Nature* 478: 395-398.
- 768 Doehlemann G, Reissmann S, Aßmann D, Fleckenstein M, Kahmann R. 2011. Two linked  
769 genes encoding a secreted effector and a membrane protein are essential for *Ustilago maydis*-  
770 induced tumour formation. *Mol Microbiol* 81: 751-766.
- 771 Doehlemann G, et al. 2009. Pep1, a secreted effector protein of *Ustilago maydis*, is required  
772 for successful invasion of plant cells. *PLoS Pathog* 5: e1000290.
- 773 Doehlemann G, et al. 2008. Reprogramming a maize plant: transcriptional and metabolic  
774 changes induced by the fungal biotroph *Ustilago maydis*. *Plant J* 56: 181-195.
- 775 Dong S, et al. 2014. Effector specialization in a lineage of the Irish potato famine pathogen.  
776 *Science* 343: 552-555.
- 777 Dutheil JY, Boussau B. 2008. Non-homogeneous models of sequence evolution in the Bio++  
778 suite of libraries and programs. *BMC Evol Biol* 8: 255.
- 779 Dutheil JY, et al. 2012. Efficient selection of branch-specific models of sequence evolution.  
780 *Mol Biol Evol* 29: 1861-1874.

- 781 Dutheil JY, et al. 2016. A tale of genome compartmentalization: the evolution of virulence  
782 clusters in smut fungi. *Genome Biol Evol* 8: 681-704.
- 783 Etuk EB, et al. 2012. Nutrient composition and feeding value of *Sorghum* for livestock and  
784 poultry: a review. *J Anim Sci Adv* 2: 510-524.
- 785 Fisher MC, et al. 2012. Emerging fungal threats to animal, plant and ecosystem health. *Nature*  
786 484: 186-194.
- 787 Franceschetti M, et al. 2017. Effectors of filamentous plant pathogens: commonalities amid  
788 diversity. *Microbiol Mol Biol R* 81: e00066-00016.
- 789 Gehrig H, Schussler A, Kluge M. 1996. *Geosiphon pyriforme*, a fungus forming  
790 endocytobiosis with *Nostoc* (cyanobacteria), is an ancestral member of the *Glomales*:  
791 evidence by SSU rRNA analysis. *J Mol Evol* 43: 71-81.
- 792 Ghareeb HA, Becker A, Iven T, Feussner I, Schirawski J. 2011. *Sporisorium reilianum*  
793 infection changes inflorescence and branching architectures of maize. *Plant Physiol* 156:  
794 2037-2052.
- 795 Giraldo MC, Valent B. 2013. Filamentous plant pathogen effectors in action. *Nat Rev*  
796 *Microbiol* 11: 800-814.
- 797 Gillespie JH. 1994. The causes of molecular evolution. Oxford: Oxford University Press.
- 798 Goulet KM, Saville BJ. 2017. Carbon acquisition and metabolic changes during fungal  
799 biotrophic plant pathogenesis: insights from *Ustilago maydis*. *Can J Plant Pathol* 39: 247-266.
- 800 Grandaubert J, et al. 2014. Transposable element-assisted evolution and adaptation to host  
801 plant within the *Leptosphaeria maculans*-*Leptosphaeria biglobosa* species complex of fungal  
802 pathogens. *BMC Genomics* 15: 891.
- 803 Grossmann S, Bauer S, Robinson PN, Vingron M. 2007. Improved detection of  
804 overrepresentation of Gene-Ontology annotations with parent child analysis. *Bioinformatics*  
805 23: 3024-3031.
- 806 Guindon S, et al. 2010. New algorithms and methods to estimate maximum-likelihood  
807 phylogenies: assessing the performance of PhyML 3.0. *Syst Biol* 59: 307-321.
- 808 Hacquard S et al. 2012. A Comprehensive Analysis of Genes Encoding Small Secreted  
809 Proteins Identifies Candidate Effectors in *Melampsora larici-populina* (Poplar Leaf Rust).  
810 *Mol Plant Microbe In* 25: 279-293.
- 811 Harrell Jr. FE. 2015. Regression Modeling Strategies. Springer Series in Statistics,  
812 Switzerland.
- 813 Haueisen J, Stukenbrock EH. 2016. Life cycle specialization of filamentous pathogens -  
814 colonization and reproduction in plant tissues. *Curr Opin Microbiol* 32: 31-37.
- 815 Hemetsberger C, et al. 2015. The fungal core effector Pep1 is conserved across smuts of  
816 dicots and monocots. *New Phytol* 206: 1116-1126.

- 817 Huang J, Si W, Deng Q, Li P, Yang S. 2014. Rapid evolution of avirulence genes in rice blast  
818 fungus *Magnaporthe oryzae*. BMC Genetics 15: 45.
- 819 Jansen G, Wu C, Schade B, Thomas DY, Whiteway M. 2005. Drag&Drop cloning in yeast.  
820 Gene 344: 43-51.
- 821 Joly DL, Feau N, Tanguay P, Hamelin RC. 2010. Comparative analysis of secreted protein  
822 evolution using expressed sequence tags from four poplar leaf rusts (*Melampsora* spp.). BMC  
823 Genomics 11: 422.
- 824 Jordan G, Goldman N. 2012. The effects of alignment error and alignment filtering on the  
825 sitewise detection of positive selection. Mol Biol Evol 29: 1125-1139.
- 826 Kämper J. 2004. A PCR-based system for highly efficient generation of gene replacement  
827 mutants in *Ustilago maydis*. Mol Genet Genomics 271: 103-110.
- 828 Kämper J, et al. 2006. Insights from the genome of the biotrophic fungal plant pathogen  
829 *Ustilago maydis*. Nature 444: 97-101.
- 830 Kazazian HH. 2004. Mobile elements: drivers of genome evolution. Science 303: 1626-1632.
- 831 Khrunyk Y, Münch K, Schipper K, Lupas AN, Kahmann R. 2010. The use of FLP-mediated  
832 recombination for the functional analysis of an effector gene family in the biotrophic smut  
833 fungus *Ustilago maydis*. New Phytol 187: 957-968.
- 834 Kretschmer M, Klose J, Kronstad JW. 2012. Defects in mitochondrial and peroxisomal  $\beta$ -  
835 oxidation influence virulence in the maize pathogen *Ustilago maydis*. Eukaryot Cell 11:  
836 1055-1066.
- 837 Kumar S, Stecher G, Suleski M, Hedges SB. 2017. TimeTree: a resource for timelines,  
838 timetrees, and divergence times. Mol Biol Evol 34: 1812-1819.
- 839 Lanver D, et al. 2017. *Ustilago maydis* effectors and their impact on virulence. Nat Rev  
840 Microbiol 15: 409-421.
- 841 Lartillot N, Lepage T, Blanquart S. 2009. PhyloBayes 3: a Bayesian software package for  
842 phylogenetic reconstruction and molecular dating. Bioinformatics 25: 2286-2288.
- 843 Laurie JD, et al. 2012. Genome comparison of barley and maize smut fungi reveals targeted  
844 loss of RNA silencing components and species-specific presence of transposable elements.  
845 Plant Cell 24: 1733-1745.
- 846 Le SQ, Gascuel O. 2008. An improved general amino acid replacement matrix. Mol Biol Evol  
847 25: 1307-1320.
- 848 Lo Presti L, et al. 2015. Fungal effectors and plant susceptibility. Annu Rev Plant Biol 66:  
849 513-545.
- 850 Löytynoja A, Goldman N. 2008. Phylogeny-aware gap placement prevents errors in sequence  
851 alignment and evolutionary analysis. Science 320: 1632-1635.



- 852 Lübberstedt T, Xia XC, Tan G, Liu X, Melchinger AE. 1999. QTL mapping of resistance to  
853 *Sporisorium reilianum* in maize. *Theor Appl Genet* 99: 593-598.
- 854 Martin FM, Uroz S, Barker DG. 2017. Ancestral alliances: Plant mutualistic symbioses with  
855 fungi and bacteria. *Science* 356: eaad4501.
- 856 Martinez-Espinoza AD, Garcia-Pedrajas MD, Gold SE. 2002. The Ustilaginales as plant pests  
857 and model systems. *Fungal Genet Biol* 35: 1-20.
- 858 Mazaheri-Naeini M, Sabbagh SK, Martinez Y, Séjalon-Delmas N, Roux C. 2015. Assessment  
859 of *Ustilago maydis* as a fungal model for root infection studies. *Fungal Biol* 119: 145–153.
- 860 Miele V, Penel S, Duret L. 2011. Ultra-fast sequence clustering from similarity networks with  
861 SiLiX. *BMC Bioinformatics* 12: 116.
- 862 Möller M, Stukenbrock EH. 2017. Evolution and genome architecture in fungal plant  
863 pathogens. *Nat Rev Microbiol* 15: 756-771.
- 864 Mueller AN, Ziemann S, Treitschke S, Aßmann D, Doehlemann G. 2013. Compatibility in  
865 the *Ustilago maydis*–maize interaction requires inhibition of host cysteine proteases by the  
866 fungal effector Pit2. *PLoS Pathog* 9: e1003177.
- 867 Munkacsı AB, Stoxen S, May G. 2007. Domestication of maize, sorghum, and sugarcane did  
868 not drive the divergence of their smut pathogens. *Evolution* 61: 388–403
- 869 Nielsen R. 2005. Molecular signatures of natural selection. *Annu Rev Genet* 39: 197-218.
- 870 Nielsen R, Yang Z. 1998. Likelihood models for detecting positively selected amino acid sites  
871 and applications to the HIV-1 envelope gene. *Genetics* 148: 929-936.
- 872 Parniske M. 2008. Arbuscular mycorrhiza: the mother of plant root endosymbioses. *Nat Rev*  
873 *Microbiol* 6: 763-775.
- 874 Petersen TN, Brunak S, von Heijne G, Nielsen H. 2011. SignalP 4.0: discriminating signal  
875 peptides from transmembrane regions. *Nat Methods* 8: 785-786.
- 876 Petit-Houdenot Y, Fudal I. (2017). Complex Interactions between Fungal Avirulence Genes  
877 and Their Corresponding Plant Resistance Genes and Consequences for Disease Resistance  
878 Management. *Front Plant Sci* 8: 1072.
- 879 Plissonneau C, et al. 2017. Using population and comparative genomics to understand the  
880 genetic basis of effector-driven fungal pathogen evolution. *Front Plant Sci* 8: 119.
- 881 Poppe S, Dorsheimer L, Happel P, Stukenbrock EH. 2015. Rapidly evolving genes are key  
882 players in host specialization and virulence of the fungal wheat pathogen *Zymoseptoria tritici*  
883 (*Mycosphaerella graminicola*). *PLoS Pathog* 11: e1005055.
- 884 Que Y, et al. 2014. Genome sequencing of *Sporisorium scitamineum* provides insights into  
885 the pathogenic mechanisms of sugarcane smut. *BMC Genomics* 15: 996.
- 886 Raffaele S, Kamoun S. 2012. Genome evolution in filamentous plant pathogens: why bigger  
887 can be better. *Nat Rev Microbiol* 10: 417-430.

- 888 Ranwez V, Harispe S, Delsuc F, Douzery EJP. 2011. MACSE: Multiple Alignment of Coding  
889 SEquences accounting for frameshifts and stop codons. PLOS One 6: e22594.
- 890 Remy W, Taylor TN, Hass H, Kerp H. 1994. Four hundred-million-year-old vesicular  
891 arbuscular mycorrhizae. PNAS 91: 11841-11843.
- 892 Romiguier J, et al. 2012. Fast and robust characterization of time-heterogeneous sequence  
893 evolutionary processes using substitution mapping. PLOS One 7: e33852.
- 894 Rouxel T, et al. 2011. Effector diversification within compartments of the *Leptosphaeria*  
895 *maculans* genome affected by Repeat-Induced Point mutations. Nat Commun 2: 202.
- 896 Rovenich H, Boshoven JC, Thomma BPHJ. 2014. Filamentous pathogen effector functions:  
897 of pathogens, hosts and microbiomes. Curr Opin Plant Biol 20: 96–103.
- 898 Sainudiin R, et al. 2005. Detecting site-specific physicochemical selective pressures:  
899 applications to the Class I HLA of the human major histocompatibility complex and the SRK  
900 of the plant sporophytic self-incompatibility system. J Mol Evol 60: 315-326.
- 901 Schipper K 2009. Charakterisierung eines *Ustilago maydis* Genclusters, das für drei neuartige  
902 sekretierte Effektoren kodiert. Philipps-Universität Marburg.
- 903 Schirawski J, et al. 2010. Pathogenicity determinants in smut fungi revealed by genome  
904 comparison. Science 330: 1546-1548.
- 905 Schneider A, et al. 2009. Estimates of positive Darwinian selection are inflated by errors in  
906 sequencing, annotation, and alignment. Genome Biol Evol 1: 114-118.
- 907 Schulz B, et al. 1990. The *b* alleles of *U. maydis*, whose combinations program pathogenic  
908 development, code for polypeptides containing a homeodomain-related motif. Cell 60: 295-  
909 306.
- 910 Schuster M, Schweizer G, Kahmann R. 2017. Comparative analyses of secreted proteins in  
911 plant pathogenic smut fungi and related basidiomycetes. Fungal Genet Biol in press.
- 912 Schuster M, Schweizer G, Reissmann S, Kahmann R. 2016. Genome editing in *Ustilago*  
913 *maydis* using the CRISPR–Cas system. Fungal Genet Biol 89: 3-9.
- 914 Sharma R, Mishra B, Runge F, Thines M. 2014. Gene loss rather than gene gain is associated  
915 with a host jump from monocots to dicots in the smut fungus *Melanopsichium*  
916 *pennsylvanicum*. Genome Biol Evol 6: 2034-2049.
- 917 Sharma R, Xia X, Riess K, Bauer R, Thines M. 2015. Comparative genomics including the  
918 early-diverging smut fungus *Ceraceosorus bombacis* reveals signatures of parallel evolution  
919 within plant and animal pathogens of fungi and oomycetes. Genome Biol Evol 7: 2781-2798.
- 920 Sikorski RS, Hieter P. 1989. A system of shuttle vectors and yeast host strains designed for  
921 efficient manipulation of DNA in *Saccharomyces cerevisiae*. Genetics 122: 19-27.
- 922 Sperschneider J, et al. 2015. Genome-wide analysis in three *Fusarium* pathogens identifies  
923 rapidly evolving chromosomes and genes associated with pathogenicity. Genome Biol Evol 7:  
924 1613-1627.

- 925 Sperschneider J, et al. 2014. Diversifying selection in the wheat stem rust fungus acts  
926 predominantly on pathogen-associated gene families and reveals candidate effectors. *Front*  
927 *Plant Sci* 5: 372.
- 928 Stergiopoulos I, de Wit PJ. 2009. Fungal effector proteins. *Annu Rev Phytopathol* 47: 233-  
929 263.
- 930 Stukenbrock EH, et al. 2011. The making of a new pathogen: insights from comparative  
931 population genomics of the domesticated wheat pathogen *Mycosphaerella graminicola* and its  
932 wild sister species *Genome Res* 21: 2157-2166.
- 933 Taniguti LM, et al. 2015. Complete genome sequence of *Sporisorium scitamineum* and  
934 biotrophic interaction transcriptome with sugarcane. *PLOS One* 10: e0129318.
- 935 Tellier A, Moreno-Gómez S, Stephan W. 2014. Speed of adaptation and genomic footprints of  
936 host-parasite coevolution under arms race and trench warfare dynamics. *Evolution* 68: 2211-  
937 2224.
- 938 Thompson JD, Plewniak F, Poch O. 1999. A comprehensive comparison of multiple sequence  
939 alignment programs. *Nucleic Acids Res* 27: 2682-2690.
- 940 Thorne JL, Kishino H, Painter IS. 1998. Estimating the rate of evolution of the rate of  
941 molecular evolution. *Mol Biol Evol* 15: 1647-1657.
- 942 Tiffin P, Moeller DA. 2006. Molecular evolution of plant immune system genes. *Trends*  
943 *Genet* 22: 662-670.
- 944 Toruño TY, Stergiopoulos I, Coaker G. 2016. Plant-pathogen effectors: cellular probes  
945 interfering with plant defenses in spatial and temporal manners. *Annu Rev Phytopathol* 54:  
946 419-441.
- 947 Wicker T, et al. 2013. The wheat powdery mildew genome shows the unique evolution of an  
948 obligate biotroph. *Nat Genet* 45: 1092-1096.
- 949 Yang Z. 1998. Likelihood ratio tests for detecting positive selection and application to  
950 primate lysozyme evolution. *Mol Biol Evol* 15: 568-573.
- 951 Yang Z, Nielsen R. 1998. Synonymous and nonsynonymous rate variation in nuclear genes of  
952 mammals. *J Mol Evol* 46:409-418.
- 953 Yang Z. 2006. *Computational Molecular Evolution*. Oxford Series in Ecology and Evolution,  
954 Oxford University Press.
- 955 Yang Z. 2007. PAML 4: phylogenetic analysis by maximum likelihood. *Mol Biol Evol* 24:  
956 1586-1591.
- 957 Zhan J, McDonald BA. 2013. Experimental measures of pathogen competition and relative  
958 fitness. *Annu Rev Phytopathol* 51: 131-153.
- 959 Zuther K, et al. 2012. Host specificity of *Sporisorium reilianum* is tightly linked to generation  
960 of the phytoalexin luteolinidin by *Sorghum bicolor*. *Mol Plant Microbe Interact* 25: 1230-  
961 1237.

962 **Tables**

963

964 **Table 1:** Gene Ontology terms significantly overrepresented in positively selected genes

965 encoding cytoplasmic proteins in *S. reilianum* and *U. hordei*

<b>Gene Ontology Id</b>	<b>Gene Ontology Description</b>	<b>Category<sup>a)</sup></b>	<b>P values<sup>b)</sup></b>	<b>Species<sup>c)</sup></b>
GO:0030532	small nuclear ribonucleoprotein complex	CC	0.023	Srr
GO:0045263	proton-transporting ATP synthase complex, coupling factor F(o)	CC	0.038 and 0.036	Srr and Srz
GO:0044425	membrane part	CC	0.047	Srr
GO:0031668	cellular response to extracellular stimulus	BP	0.015 and 0.013	Srr and Srz
GO:0051186	cofactor metabolic process	BP	0.015	Srr
GO:0042594	response to starvation	BP	0.017 and 0.012	Srr and Srz
GO:0009267	cellular response to starvation	BP	0.020 and 0.014	Srr and Srz
GO:0006790	sulfur compound metabolic process	BP	0.022	Srr
GO:0051301	cell division	BP	0.023	Srr
GO:0006777	Mo-molybdopterin cofactor biosynthetic process	BP	0.027	Srr
GO:0009605	response to external stimulus	BP	0.027 and 0.012	Srr and Srz
GO:0043545	molybdopterin cofactor metabolic process	BP	0.034	Srr
GO:0043413	macromolecule glycosylation	BP	0.036	Srr
GO:0022402	cell cycle process	BP	0.037	Srr
GO:0051189	prosthetic group metabolic process	BP	0.039	Srr
GO:0006139	nucleobase-containing compound metabolic process	BP	0.012	Srz
GO:0016070	RNA metabolic process	BP	0.023	Srz
GO:1901360	organic cyclic compound metabolic process	BP	0.016	Srz
GO:0006725	cellular aromatic compound metabolic process	BP	0.024	Srz
GO:0046483	heterocycle metabolic process	BP	0.023	Srz
GO:0035383	thioester metabolic process	BP	0.041	Srr
GO:1902589	single-organism organelle organization	BP	0.048	Srr
GO:0015074	DNA integration	BP	0.039	Uh
GO:0006259	DNA metabolic process	BP	0.023	Uh
GO:0010181	FMN binding	MF	0.047 and 0.022	Srr and Srz
GO:0030515	snoRNA binding	MF	0.021	Srz
GO:0016491	oxidoreductase activity	MF	0.028	Srz
GO:0016853	isomerase activity	MF	0.029	Uh

966

967

968 <sup>a)</sup> CC, Cellular Component; BP, Biological Process; MF, Molecular Function.

969 <sup>b)</sup> calculated by Fisher's classic test with Parent-Child correction. Only entries with  $P$  value  $\leq$   
970 0.05 are shown.

971 <sup>c)</sup> Species in which GO terms were found enriched. Srr, *S. reilianum* f. sp. *reilianum*; Srz, *S.*

972 *reilinaum* f. sp. *zeae*; Uh, *U. hordei*.

973

974

975

976

977

978

979

980

981

982

983

984 **Table 2:** Positively selected genes that were deleted in *S. reilianum* f. sp. *zear* and their selection criteria

Family	Gene Id	Gene description	$d_N/d_S$	Species with detected positive selection <sup>a)</sup>	Number of Paralogs in Srz <sup>b)</sup>	Virulence phenotype of candidate gene deletion	Closest ortholog in <i>U. maydis</i> <sup>c)</sup>
FAM001428	<i>sr10529</i>	conserved hypothetical protein	31.1469	Srz and Srr	0	virulence abolished	UMAG_01375 ( <i>pit2</i> ) <sup>6)</sup>
FAM005472	<i>sr10059</i>	conserved hypothetical <i>Ustilaginaceae</i> -specific protein	6.53881	Srz and Srr	0	virulence unaffected	UMAG_05306 (cluster 19A) <sup>7)</sup>
FAM000532	<i>sr10182</i>	conserved hypothetical protein	1.57473	Srr	10 <sup>3)</sup>	virulence unaffected	UMAG_00492
FAM002067	<i>sr12968</i>	conserved hypothetical protein	37.9007	Srr	0	virulence unaffected	UMAG_02006
FAM003728	<i>sr14558</i>	conserved hypothetical protein	24.355	Srz	0	virulence unaffected	UMAG_03564
FAM004113	<i>sr14944</i>	conserved hypothetical <i>Ustilaginaceae</i> -specific protein	4.30527	Srz and Srr	0	virulence unaffected	UMAG_04034 (cluster 11-16) <sup>8)</sup>
FAM003465	<i>sr14347</i>	conserved hypothetical protein	544.37	Srz	5 <sup>4)</sup>	virulence unaffected	UMAG_03349
FAM001868	<i>sr12897</i>	conserved hypothetical protein	infinite <sup>1)</sup>	Srr	0	virulence unaffected	UMAG_01820
FAM000842	<i>sr12084</i>	conserved hypothetical protein	infinite <sup>2)</sup>	Srz	2 <sup>5)</sup>	virulence unaffected	UMAG_00792 (cluster 1-32) <sup>8)</sup>

- 985 <sup>a)</sup> species are *S. reilianum* f. sp. *zeae* (Srz) and *S. reilianum* f. sp. *reilianum* (Srr)
- 986 <sup>b)</sup> based on blastp search with an e-value cutoff of 0.001
- 987 <sup>c)</sup> based on blastp search
- 988 <sup>1)</sup> infinity due to low value of  $d_s$
- 989 <sup>2)</sup> infinity due to long branch for *sr12085*, a species-specific duplicate in *S. reilianum* f. sp.  
990 *zeae*
- 991 <sup>3)</sup> the ten paralogs include: *sr13431*, *sr11876*, *sr16607*, *sr11405*, *sr10621*, *sr16723*, *sr16877*,  
992 *13293*, *sr11163.2* and *sr15970*
- 993 <sup>4)</sup> the five paralogs include: *sr12257*, *sr11661*, *sr13976*, *sr14607* and *sr11273*
- 994 <sup>5)</sup> the two paralogs include: *sr12085* and *sr12086*
- 995 <sup>6)</sup> as described in Doehlemann et al., 2011 and Mueller et al., 2013
- 996 <sup>7)</sup> as described in Kämper et al., 2006
- 997 <sup>8)</sup> as described in Schirawski et al., 2010
- 998

## 999 **Figure legends**

1000 **FIG. 1.** Phylogeny, divergence estimates and number of genes under positive selection in five  
1001 related smut fungal species parasitizing different host plants. A) Chronogram of the five  
1002 fungal pathogens as estimated under a relaxed molecular clock. Boxes represent 95%  
1003 posterior intervals, with corresponding values indicated below. B) Pairwise sequence  
1004 differences, for both the non-coding genome and the proteome (non-synonymous differences).  
1005 C) Number of positively selected genes on each terminal branch (total number of genes and  
1006 genes predicted to encode a secreted protein).

1007

1008 **FIG. 2.** Virulence phenotypes of single deletion mutants of positively selected genes in *S.*  
1009 *reilianum* f. sp. *zaae*. Plants of the maize variety ‘Gaspé Flint’ were infected with the  
1010 solopathogenic strain JS161 or independent deletion mutants of candidate genes as indicated  
1011 below each bar. Deletion of *sr10529* led to a strong reduction in virulence (A). In contrast,  
1012 deletion of the candidate genes *sr12968* (B), *sr14944* (C), *sr10059* (D), *sr10182* (E), *sr14558*  
1013 (F), *sr14347* (G), *sr12897* (H), and *sr12084* (I) did not alter virulence. Symptoms were scored  
1014 about 9 weeks post infection and categorized according to severeness as illustrated in the  
1015 legend below the bar plots. Results are shown as mean of three independent experiments in  
1016 relation to the total number of infected plants, which is indicated above each bar (n). Note that  
1017 strains JS161Δ*Sr10529* #G4 and #G5 (A) were only infected in one replicate.

1018

1019

1020

1021



1022 **FIG. 3.** Distribution of positively selected amino acids in the cysteine protease inhibitor Pit2.  
1023 The alignment shows the protein sequences of orthologues in *U. hordei* (UHOR\_02064), *U.*  
1024 *maydis* (UMAG\_01375), *S. scitamineum* (SPSC\_03677), *S. reilianum* f. sp. *zeae* (sr10529)  
1025 and *S. reilianum* f. sp. *reilianum* (srs\_10529). Sites under positive selection detected by a  
1026 branch-site model are indicated by colored bold letters. Residues colored in red indicate  
1027 positive selection detected in the respective species and purple residues indicate sites found  
1028 under positive selection in both species. The yellow shaded area is orthologous to the  
1029 previously identified conserved PID14 domain, which is required and sufficient for inhibition  
1030 of a group of papain-like cysteine proteases. Green sequences indicate secretion signal  
1031 peptides and bold numbers above the alignment indicate positions in UHOR\_02064.

1032 **List of supplementary tables**

1033 **Supplementary table S1:** Sources of genomic data for the five smut fungi species  
1034 investigated  
1035

1036 **Supplementary table S2:** Results of the molecular dating analysis

1037 **Supplementary table S3:** Prediction of secretion, Gene Ontology Terms and  $d_N / d_S$  ratios for  
1038 all 33,940 proteins in five smut fungi  
1039

1040 **Supplementary table S4:** List of strains of *S. reilianum* f. sp. *zeae* used in the present study

1041 **Supplementary table S5:** List of primers used in the present study

1042 **Supplementary table S6:** Grouping of 33,940 proteins of five compared smut fungi species  
1043 in 8,761 families  
1044

1045 **Supplementary table S7:** Results of a linear model illustrating the associations between gene  
1046 duplications, positive selection and candidate effector genes  
1047  
1048

1049

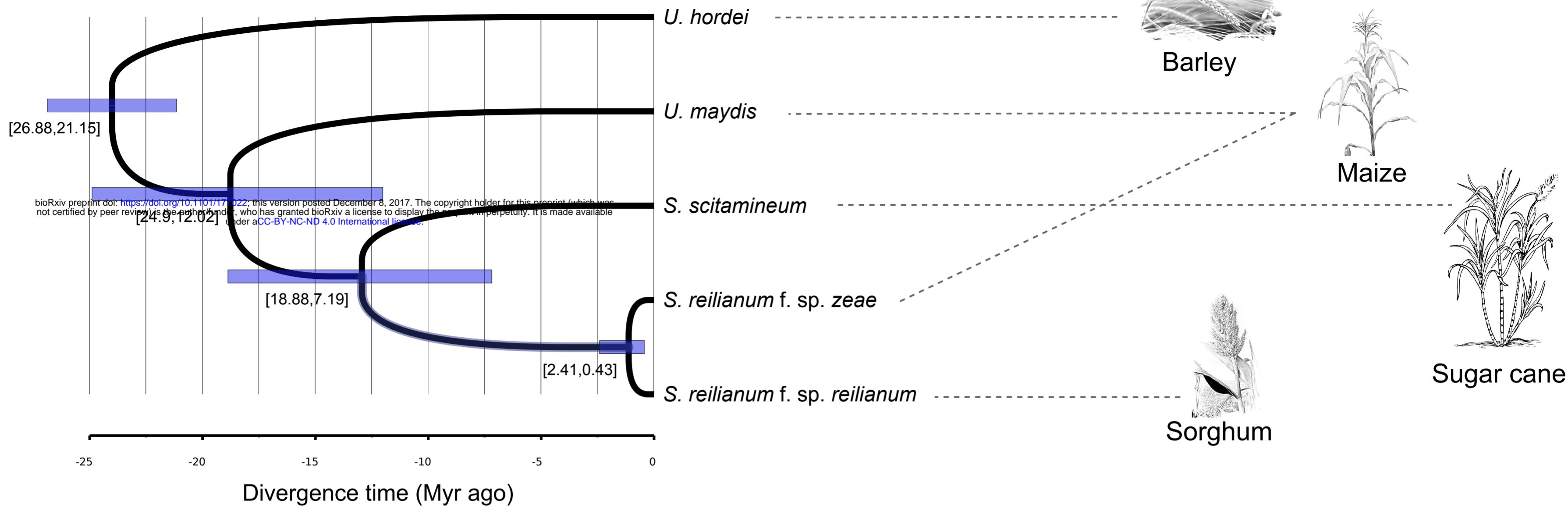
1050 **List of supplementary figures**

1051 **Supplementary figure 1.** Number of families consisting of 1:1 orthologues in relation to  
1052 varying settings for coverage and identity in the clustering program SiLiX. The maximum  
1053 number of families containing 1:1 orthologues can be obtained with a coverage between 5 %  
1054 and 45 % and an identity of 40 %.

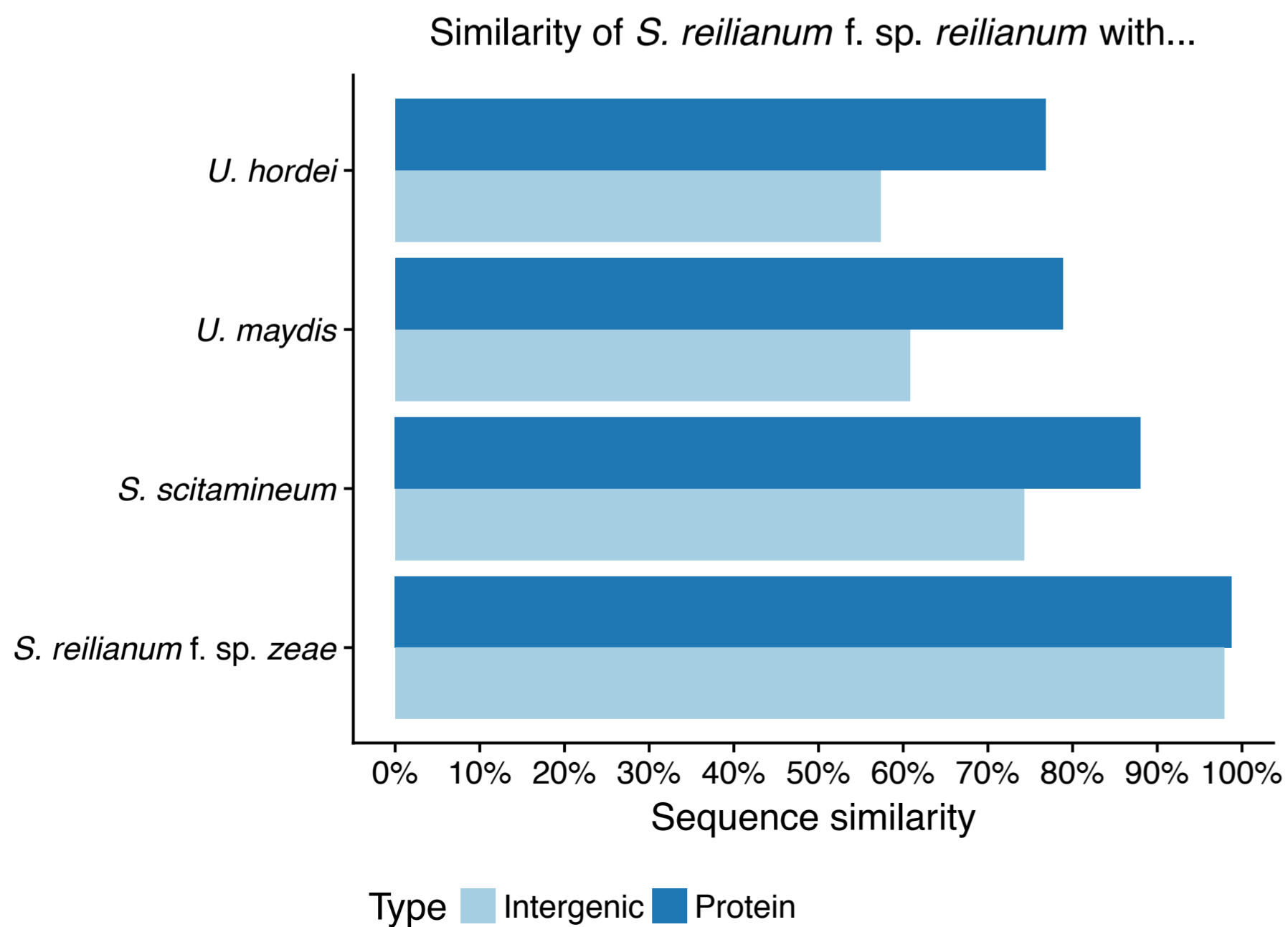
1055

1056 **Supplementary figure 2.** Trace of the Monte-Carlo Markov chains for 3 gene samples (see  
1057 Methods). Vertical lines show the burning phase (10,000 iterations)

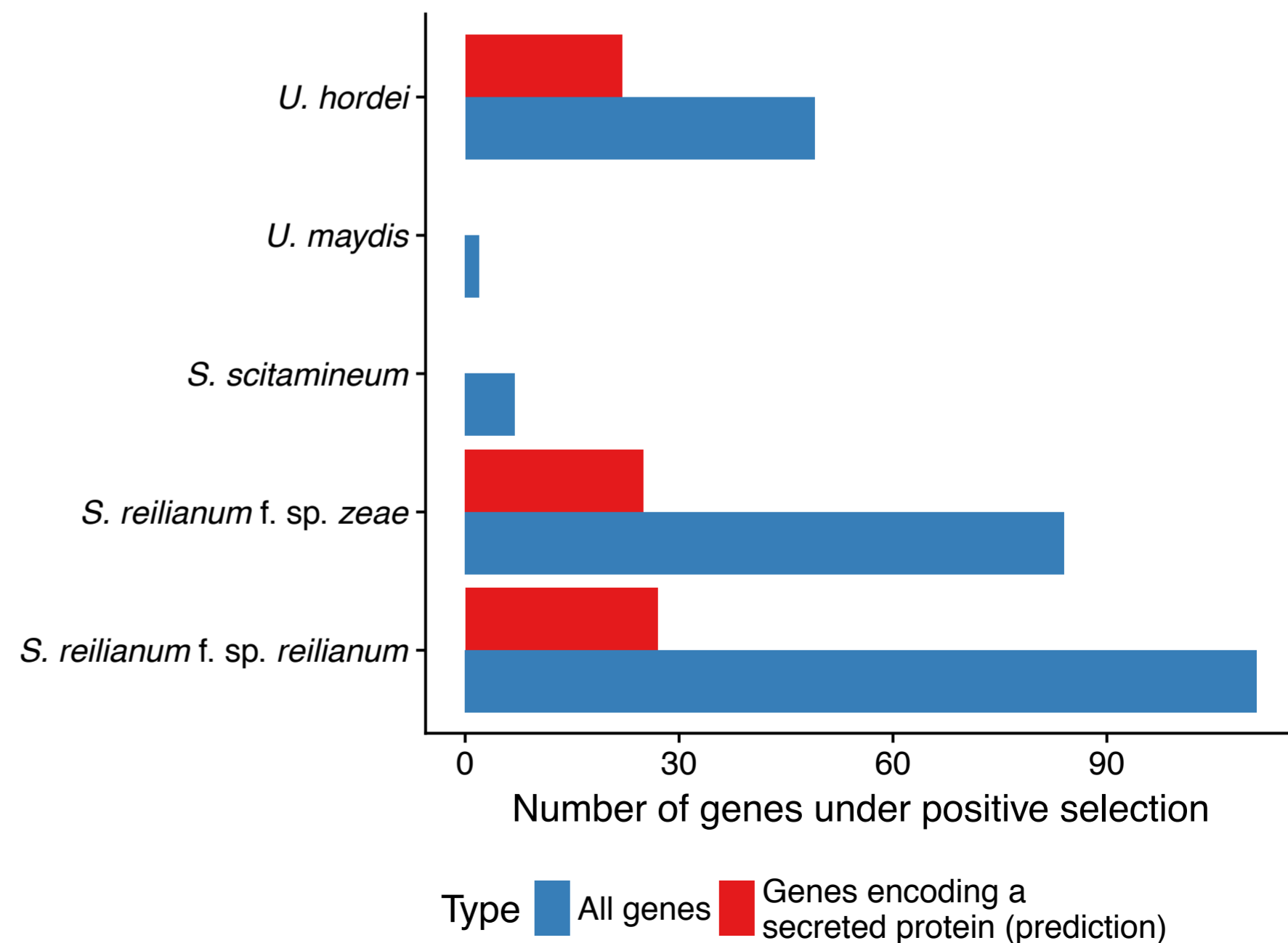
A

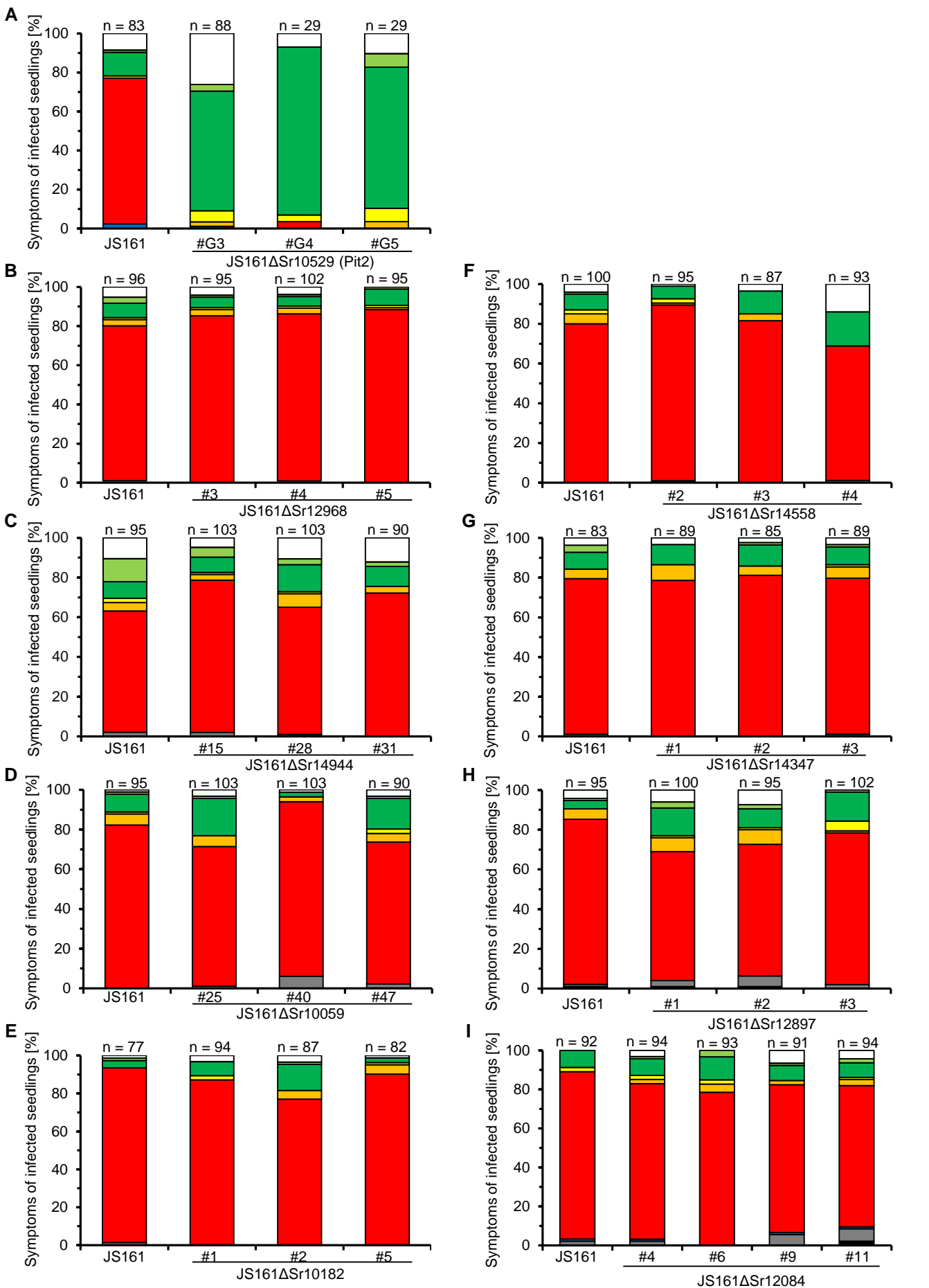


B



C





plant without ears
  healthy ears  $\leq$  1 cm
  healthy ears  $>$  1 cm
  spiky ears
  phyllody in ears  $\leq$  1 cm
  phyllody in ears  $>$  1 cm
  phyllody in tassels
  spore formation
  dead plants

20

40

UHOR_02064	<b>MLHYLGRLFLVAALAVACLR</b>	<b>PATQ</b> ---NRPLRRAIV----	-GDNNDNYITKLHRRWYFLW
UMAG_01375	<b>MLFRSAFVLLIVAFASACLV</b>	<b>QHVQA</b> I---PVRRSLSTDAS	M----SSAAGKLNRRWWFGF
SPSC_03677	<b>MLVHSAP-AFIATLVALCLA</b>	<b>QHVQA</b> IQLPAIRRSLTHNDD	A-----ANLERRWFWNF
srs_10529	<b>MLVHSAR-AFVAALL-LGLV</b>	<b>LHVHA</b> IQMPAMRRSLSSHAD	AGAAGGSTLGKLLARRWFFNF
sr10529	<b>MLVHSAR-AFVAALL-LGLV</b>	<b>LHVHA</b> --MPAMRRSLSSHAD	AGAAGGSTLGKLLARRWFF <b>DF</b>

60

80

100

UHOR_02064	PGSLAPKPPREGEEHKIIYA	DWIVHHDPAYNNSNVQKEIEL	ARLQNPTFIQVSVGESSSSS
UMAG_01375	TGSLGKEPDNGQVQIKIIPD	ALI IKNPPANKDDLNKLIEN	LKRKHPRFKTVVMPTDPNGD
SPSC_03677	GSSLGRSPDNN---ALIVPE	DMIKKHTAALVTEWQTYLNE	MHRQHPNWKRIDWRDDGPAG
srs_10529	GGSL <b>APLDAVP</b> ---I <b>FE</b> IP <b>K</b>	<b>SLIK</b> <b>THKP</b> AEV <b>T</b> <b>KWEV</b> <b>FLQR</b>	VHR <b>K</b> HPDW <b>THVHWT</b> <b>T</b> DGP <b>VG</b>
sr10529	GG <b>A</b> L <b>SRWDVAP</b> ---IL <b>R</b> IPE	<b>DVA</b> <b>KAH</b> <b>SRAEV</b> <b>AR</b> WEVYLE <b>R</b>	VHR <b>E</b> HPDW <b>QYVHWT</b> <b>D</b> <b>NGPIG</b>

120

UHOR_02064	SSSSSKKS-----	<b>120</b>
UMAG_01375	VVIWE-----	<b>118</b>
SPSC_03677	FARWESEKQGRSH	<b>121</b>
srs_10529	YK <b>G</b> H-----	<b>119</b>
sr10529	YKSH-----	<b>117</b>